

## CHAPTER 2: MESOPOROUS SILICA MCM-41 (Si-MCM-41)

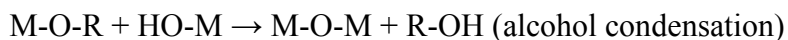
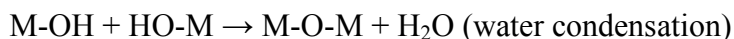
### 2.1 Introduction

Microporous and mesoporous solids [1] have found great utility as catalysts and sorption media because of their large internal surface area. Examples of mesoporous solids include silica gel [2] and layered materials [3-4], but the pores in these materials are irregularly spaced and pore sizes are broadly distributed [5]. Recently, highly uniform mesoporous materials such as M41S [6-7] and FSM-16 [8-9] have been reported and shown to contain a narrow distribution of monodisperse pore sizes. The common feature of these two groups of materials is the use of cetyltrimethylammonium cations and a wide range of silica sources during their preparation, although FSM-16 is conventionally obtained from the clay mineral, kanemite.

The superstructures of the M41S family are designated MCMs, an acronym for Mobil's Composition of Matter, and are respectively MCM-41 (hexagonal), MCM-48 (cubic) as well as MCM-50 (lamellar). The hexagonal structure, MCM-41, is by far the most studied member of this family of mesoporous materials. MCM-41 combines a myriad of attractive properties including highly ordered pore systems with tunable pore diameters (in the range 2-10 nm), large pore volumes, high hydrocarbon sorption capacities, high BET surface areas and thermal stability, as well as a high density of surface silanols. These characteristics make MCM-41 a promising option for use as catalyst, catalyst support, adsorbent and for guest-host chemistry. Reliable characterization of the porous MCM-41 structure requires the use of three independent techniques [10], namely XRD, TEM and nitrogen adsorption isotherms. The microstructure of MCM-41 under HRTEM shows a regular array of hexagonal channels running parallel to each other, and together with XRD patterns, which shows a prominent (100) reflection peak and additional higher order peaks in the range  $2^\circ \leq 2\theta \leq 7^\circ$ , can provide conclusive evidence about the quality of the synthesized material (*See chapter 1 for an extended introduction to MCM-41*).

### 2.1.1 Synthesis of MCM-41

The initial syntheses of M41S materials involved the so-called ‘liquid-crystal templating’ [6-7], in which organized micelles of cationic alkyltrimethylammonium surfactants acted as templates to direct the mesoporous structure formation by electrostatic interactions with anionic silicate precursors at 150 °C and high pH. Sol-gel synthesis has also been widely used as a versatile method for obtaining these mesoporous silicas and aluminosilicates. The sol-gel chemistry is actually the preparation of ceramic materials (e.g. glasses) by preparation of a sol, gelation of the sol, and subsequent removal of the solvent [11-12]. This process allows the synthesis of ceramic materials of high purity and homogeneity by means of preparation techniques different from the traditional processes of fusion of oxides. It occurs in liquid solutions of organometallic precursors (e.g. TMOS, TEOS, Zr(IV)-Propoxide, Ti(IV)-Butoxide, etc.), which, by means of hydrolysis and condensation reactions, lead to the formation of a new phase:



with M = Si, Zr, Ti, etc. The fundamental property and advantage of the sol-gel process is that it is possible to generate the ceramic materials at a temperature close to room temperature.

A number of synthetic factors affecting the quality of the MCM-41 mesoporous materials under hydrothermal synthesis have been investigated. Examples of such factors are gel aging, gel pH, and gel molar composition as well as surfactant counter ions: Beck et al [7] have studied the effect of the alkyl chain length of the surfactant used to template the synthesis, and observed that the pore size increases with an increase in the surfactant alkyl chain length ( $8 \leq n \leq 16$  in  $\text{C}_n\text{H}_{2n+1}(\text{CH}_3)_3\text{NBr}$ ). These authors

further observed that addition of bulky organics (e.g. mesitylene) to the synthesis gel also resulted in the expansion of the pores of the final material. In a related study, Vartuli et al [13] investigated the effect of the silicon to surfactant molar ratio in the synthesis gel, and found that MCM-41 could be obtained if the (Sur/Si) ratio is less than 1 (see Table 1.1 in chapter 1).

The effect of the pH of the synthesis gel was also investigated [14], and this study has demonstrated that the optimum pH value for a good quality MCM-41 is about 9-10. In addition to this pH adjustment, the inclusion of the  $\text{SO}_4^{2-}$  ion in the synthesis recipe of Si-MCM-41 was found to lead to a further improvement in the long-range order of the resulting material [14]. Another study by Cheng et al [15] has investigated the effect of temperature and time on the synthesis of MCM-41. This study demonstrated that the optimum parameters for the preparation of the best quality [Si]-MCM-41 was a gel of molar composition  $\text{SiO}_2$ : 0.19 TMAOH: 0.27 CTABr: 40  $\text{H}_2\text{O}$ , aged at 20 °C for 24 h followed by hydrothermal treatment at 150 °C for 48 h. These findings are contrary to those reported by Monnier et al [16], that hexagonal MCM-41 is already present at the beginning of the synthesis when carried out at 100 and 150 °C, and the yield is maximum after 48-72 h synthesis. At 150 °C, the hexagonal phase is transformed into the lamellar or amorphous phase after 96 h. For longer reaction times, the amorphous phase is the major product. In the same work by Cheng et al [15], it was reported that highly basic gels favour the lamellar product and when the gel pH is weakly basic, the quality of the MCM-41 is lower as insufficient TMAOH is available to dissolve the silica. This work reported the first observation of the (300) peak and unusually well-resolved (110) and (200) peaks in the XRD pattern of purely siliceous MCM-41. The high synthesis gel pH effect was further substantiated by Wang and Kabe [17], who obtained good Si-MCM-41 in the pH range from 11.5 to 10.0, and observed that the material prepared at pH 12.0 resembled a lamellar meso-phase (i.e. with no distinct X-ray diffraction peaks after calcination).

In other developments, the quality of the Si-MCM-41 was improved (i) by restricting calcined mesoporous silica via a secondary recrystallization in which primary MCM-41 serves as a silica source for the next hydrothermal synthesis [18-19], (ii) by the delayed neutralization method in which the highly basic synthesis gel made from water glass and CTAB ( $C_{16}$ TMAB) is titrated with an acid solution to pH 10 [20-22], (iii) by the use of a mixture of surfactants as templates, and (iv) by multiple acid titration during the course of the synthesis [23-26].

The aim of the present study was to optimize the synthesis conditions for the preparation of pure silica MCM-41 in order to obtain these materials with high reproducibility. Good quality Si-MCM-41 materials, because of their catalytically-attractive properties, are expected to provide excellent support media for the preparation of supported transition metal catalysts. As a starting point to the work in this chapter, the literature was surveyed to select a starting point for experimentation of the various sol-gel parameters: metal salt (or alkoxide), catalysis condition and concentration ratios of the precursor materials, and heat treatment of the final as-synthesized Si-MCM-41. The silica sources used in this study were water-glass (sodium silicate), tetraethyl orthosilicate (TEOS), fumed silica, a mixture of water glass and fumed silica, as well as calcined Si-MCM-41 in the case of secondary synthesis. Because of the lack of hydrothermal stability in the pure silica form of MCM-41, the choice of its preparation method is crucial in that it should result in hydrothermally durable materials. In this work, several ideas have been combined in the synthesis of Si-MCM-41, but we have predominantly adopted the “delayed neutralization” approach used by Lin et al [20-22]. Synthesis parameters such as aging time, crystallization time, crystallization temperature, synthesis gel surfactant to silica molar ratio, synthesis gel pH, silica source, surfactants of different alkyl chain lengths and addition of auxiliary species into the synthesis gel, have been optimized to afford good-quality Si-MCM-41 with enhanced structural integrity. In the preparations, the reaction mixture comprising sodium silicate, cetyltrimethylammonium bromide (CTAB), and either distilled or de-ionized water was first homogenized under magnetic stirring and

then autoclaved for various lengths of time at various temperatures. Room temperature synthesis was also performed to gain some insight into the extent of crystallization. The quality of the resulting Si-MCM-41 was deduced from XRD patterns (by the intensity of the  $d_{100}$  peak), HRTEM images and the BET surface areas. These materials were used as benchmarks for Fe- and Co-containing MCM-41 materials reported in chapter 3.

## 2.2 Experimental Section

### 2.2.1 Starting Materials (Chemicals, stock solutions and solvents)

All chemicals were used without further purification. Water-glass or sodium silicate (25.5-28.5 %  $\text{SiO}_2$ , 7.5-8.5 %  $\text{Na}_2\text{O}$ ,  $d = 1.37$  g/ml) was purchased from Merck, and was used as a silica source. Other silica sources included tetraethyl orthosilicate (TEOS) from Aldrich (98 %), fumed silica (Aerosil 200, Degussa) and Si-MCM-41 synthesized in this study. The cationic surfactants cetyltrimethylammonium bromide (CTAB or  $\text{C}_{16}\text{TMAB}$ ) and tetradecyltrimethylammonium bromide (TDTMAB or  $\text{C}_{14}\text{TMAB}$ ) were both purchased from Aldrich (98 % purity). Both distilled and deionized water were used as solvents and 1 M aqueous solutions of  $\text{H}_2\text{SO}_4$  or  $\text{HNO}_3$  were used to control the pH of the synthesis gel prior to aging at room temperature or hydrothermal treatment.

### 2.2.2 Synthesis of the Si-MCM-41 material (Procedure)

The synthesis of pure silica MCM-41 reported in this study was carried out in sealed bottles (polyethylene or polypropylene). The polyethylene bottles were used for room temperature synthesis whereas the polypropylene bottles were used for syntheses above room temperature. For the high temperature synthesis, the polypropylene (PP) bottle was loaded into a 2 L stainless steel autoclave partially filled with water to generate steam pressure. Although most of the syntheses were performed under static

(unstirred) conditions, some were performed under stirred conditions as described below:

### ***2.2.2.1 Unstirred Synthesis of Si-MCM-41***

#### *Room Temperature Synthesis of Si-MCM-41*

To a clear aqueous solution of cetyltrimethylammonium bromide (CTAB) was added a water-glass solution dropwise under magnetic stirring to give a gel with the typical molar composition

3.50 SiO<sub>2</sub> : Na<sub>2</sub>O : 1.44 CTAB : (221-425) H<sub>2</sub>O

After all the required water glass was added, the resulting gel was stirred at room temperature for 10 minutes before adjusting the pH to 10 with a dilute acid (H<sub>2</sub>SO<sub>4</sub> or HNO<sub>3</sub>) solution. After adjusting the pH, the synthesis mixture was stirred for 30 more minutes in order to attain homogeneity. The resulting homogenized synthesis gel was transferred to either a polyethylene (PE) or polypropylene (PP) bottle (with a tight sealing screw cap), and then allowed to age statically at room temperature for various lengths of time to allow crystallization to take place. The solid product was then recovered by filtration, washed with copious amounts of distilled/deionized water until the filtrate tested negatively for the anions Br<sup>-</sup> (using Ag<sup>+</sup>(aq) solution) and either SO<sub>4</sub><sup>2-</sup> (using Ba<sup>2+</sup>(aq) solution) or NO<sub>3</sub><sup>-</sup> (brown ring test), depending on the acid used for pH adjustment. After drying at room temperature, the as-synthesized Si-MCM-41 was calcined at 560 °C for 6 h to yield the mesoporous material.

#### *Hydrothermal Synthesis of Si-MCM-41*

The synthesis gel was prepared as in the room temperature synthesis above, with the gel composition kept the same. After loading the well-mixed synthesis gel into a PP

bottle and sealing with the screw cap, the PP bottle and its contents were placed in a 2 L stainless steel autoclave half-filled with water. The autoclave was then heated statically under autogeneous pressure of 1 bar to temperatures of 75-120 °C. The hydrothermal treatment time was varied. (Note that the use of temperatures above 120 °C was limited by the melting point of the PP bottle, i.e. > 120 °C). After synthesis, the solid product was recovered by suction filtration using a Buchner funnel. It was then washed several times with distilled water until a negative Br<sup>-</sup> ion test (test with Ag<sup>+</sup>) and a negative SO<sub>4</sub><sup>2-</sup> test (test with Ba<sup>2+</sup>) when sulphuric acid was used to adjust the pH. When 1 M HNO<sub>3</sub> was used to adjust the pH of the synthesis mixture, the washings were tested for the NO<sub>3</sub><sup>-</sup> ions by the brown ring test using ferrous sulphate and concentrated sulphuric acid. After washing, the material was dried at ambient temperature and then calcined under static air at 560 °C for 6 h. Optimization of the synthesis conditions was achieved by varying the temperature, synthesis time and reactant ratios as well as silica sources. Since the polypropylene bottle showed some deformation after hydrothermal treatment at 120 °C, 100 °C was chosen as the synthesis temperature of the other materials unless stated otherwise. The reproducibility of Si-MCM-41 synthesis at 100 °C over two days is shown in the figure below:

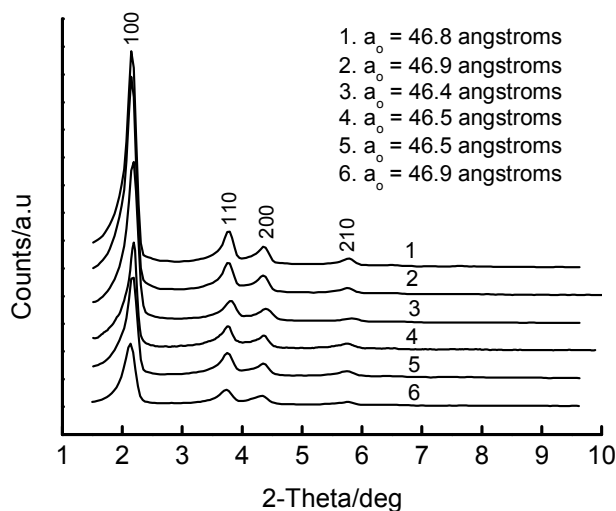


Figure 2.1. XRD patterns of Si-MCM-41 samples: Different batches prepared on different days using gels of the same composition (mean  $a_0 = 46.7$  Å).

### ***2.2.2.2 Stirred Synthesis of Si-MCM-41***

In this method, the synthesis gel with composition similar to the one in the preceding section was used, except that the silica source was a mixture of water-glass and TEOS (i. e., the total SiO<sub>2</sub> content was fixed to yield the molar composition given in section 2.2.2.1). The variable in these syntheses was the amount of water-glass added to a fixed amount of TEOS, in which sodium silicate served both as a gelling agent (because of its high pH) and as a SiO<sub>2</sub> contributor to the total SiO<sub>2</sub> content (depending on its amount). After homogenizing by magnetic stirring, the gel was allowed to age statically at room temperature for 21 hours prior to hydrothermal treatment. The hydrothermal synthesis was carried out at 80 °C for 6 h under magnetic stirring in PP bottles. After recovering the solid product by filtration, it was washed several times with deionized water until a negative Br<sup>-</sup> ion test was achieved. The resulting material was then dried at ambient and calcined at 500 °C (5 °C/min) for 12 h. The quantity R<sub>SiO<sub>2</sub></sub>, defined to represent the ratio of the SiO<sub>2</sub> contribution from TEOS to that from water-glass was used to report characterization data, i.e., R<sub>SiO<sub>2</sub></sub> = mol SiO<sub>2</sub> (TEOS)/mol SiO<sub>2</sub> (water-glass).

### **2.2.3. Characterization of the Si-MCM-41**

#### ***2.2.3.1 X-ray Powder Diffraction***

The XRD patterns of these materials were recorded on a Philips PW 1710 Automated Powder Diffractometer using a graphite monochromator-filtered Cu K<sub>α</sub> radiation ( $\lambda = 0.15406$  nm), at a generator tension of 40 kV and generator current of 20 mA. XRD patterns for the siliceous MCM-41 were recorded in the range  $1.5^\circ < 2\theta < 10^\circ$  using a step size of  $0.02^\circ$  and 1 s per step, i.e., at a scan speed of  $0.02^\circ/\text{s}$ . To allow for low angle measurements, the  $0.1^\circ$  receiving slit in the diffractometer was replaced by a  $0.25^\circ$  one.

XRD data were quantified in terms of XRD patterns and lattice parameters ( $a_0$ ), calculated from the d-spacing of the most intense (100) peak in the XRD pattern of Si-MCM-41, using the formula  $a_0 = 2 d_{100}/\sqrt{3}$ . The lattice parameter  $a_0$  represents the distance between two adjacent pore centres in the MCM-41-type material, and includes the pore wall.

### ***2.2.3.2 BET surface area measurement***

The BET (Brunauer, Emmett, Teller) method of calculating specific surface area from an adsorption isotherm is reliable and widely used. Surface area measurements were performed on a Micromeritics ASAP 2010 surface analyzer by adsorbing gaseous  $N_2$  at liquid nitrogen temperature. The samples (0.2-0.3 g) were degassed at 300 °C until a vacuum pressure of 2-4  $\mu\text{m Hg}$  was obtained, prior to analysis. A relative pressure range ( $P/P_0$ ) of 0.05-0.25 was used in the analysis.

### ***2.2.3.3 HRTEM studies of Si-MCM-41***

The microstructure of Si-MCM-41 was investigated using a JEOL 2010 high resolution transmission electron microscope (HRTEM), using an accelerating voltage of 200 kV. In the sample preparation, Si-MCM-41 materials were ground to a thin paste in ethyl alcohol, mounted on a carbon-coated copper grid by dipping the grid in the paste, air-dried at ambient temperature and then loaded into the microscope chamber for analysis.

## **2.3. Results and Discussion**

The structural properties of MCM-41-type materials prepared in this study have been investigated by using XRD and HRTEM, because these techniques can provide conclusive evidence about the structural integrity of the mesoporous materials. XRD was used to confirm the identity, crystallinity and purity of zeolite-type materials,

whereas HRTEM was used to elucidate the microstructure. BET is also another physicochemical technique, based on adsorption isotherms, which can provide information about the surface and textural properties of mesoporous materials. The results obtained from these characterization techniques will be discussed separately, and classed according to the synthesis temperature in each case.

### **2.3.1 Structural (Bulk) Characterization of Si-MCM-41 (XRD)**

The bulk (structural) properties of the synthesized Si-MCM-41 materials have been characterized using X-ray powder diffraction. The XRD pattern of MCM-41 typically shows three to five reflections between  $2\theta = 2^\circ$  and  $7^\circ$ . The diffractograms and/or the calculated lattice parameters of these materials (both calcined and uncalcined) are reported and discussed below. A comparison of the structures of pure silica materials prepared at ambient temperature with those of similar materials prepared at higher temperatures is also reported.

#### ***2.3.1.1 Room Temperature Synthesis***

The first successful synthesis of Si-MCM-41 in our laboratory was achieved by allowing a well-mixed synthesis gel composed of sodium silicate, cetyltrimethylammonium bromide (CTAB), and distilled/deionized water (gel pH pre-adjusted to 10) to age statically in a sealed polyethylene (PE) bottle at room temperature for 47 days. The XRD patterns of Si-MCM-41 materials synthesized at ambient temperature over an extended (47 days) aging period, with different solvent qualities, are shown in Figure 2.2 below:

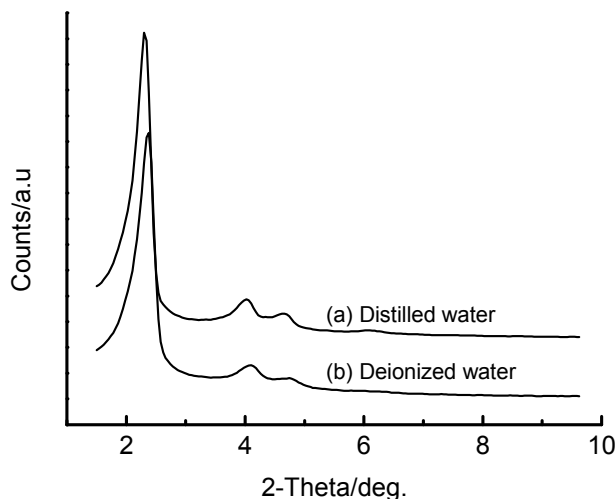


Figure 2.2. XRD patterns of Si-MCM-41 materials synthesized at room temperature for 47 days. Replicate syntheses were done using distilled water and deionized water as solvent media.

The XRD patterns of these materials (Figure 2.2 above) show features characteristic of mesoporous silica, i.e., three peaks that can be indexed on a hexagonal unit cell to (100), (110) and (200) by analogy with literature reports. The figure shows that the (100) peak of the material synthesized in deionized water is shifted to the right relative to that of the similar material prepared in distilled water. This implies that the latter material possesses slightly larger pores than the former since the pore size is related to the lattice parameter ( $a_0$ ) in these materials. The existence of higher order peaks, (110) and (200), in these materials suggests a degree of order or regularity in the arrangement of the hexagonal pores. Thus it is possible to obtain mesoporous materials with high order in the pores via a room temperature synthesis approach, although the initial materials reported by Mobil researchers [6, 7] were obtained under hydrothermal conditions. Distilled water is thus a good solvent for the synthesis of Si-MCM-41 under these conditions. XRD patterns of representative pure silica MCM-41 materials prepared at room temperature over different time periods are shown in the Figure 2.3 below:

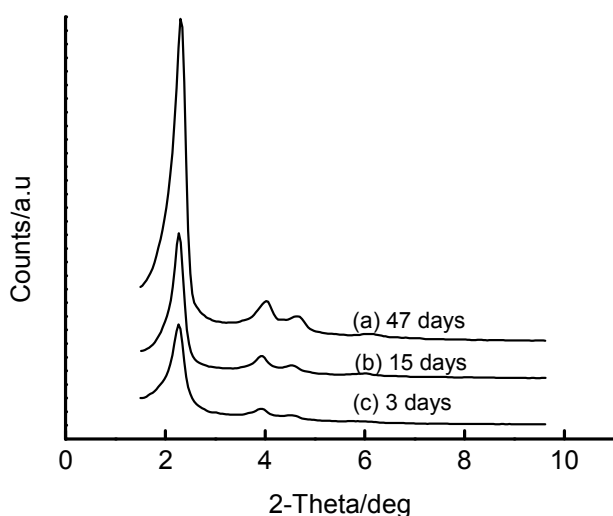


Figure 2.3. XRD patterns of some Si-MCM-41 materials prepared at room temperature

The long range order of these materials (deduced from the presence of well-resolved higher order peaks in addition to the (100) peak) is found to improve with an increase in the synthesis time under these conditions. This observation may suggest that at ambient temperature, the hydrolysis and condensation steps required to build up the network structure of the silica are slow. Although synthesis over 47 days results in a material with excellent mesoporous properties, such a duration in synthesis is not viable on an industrial scale. Therefore, most of the room temperature syntheses reported in this thesis were limited to 5 days, unless stated otherwise. Table 2.1 below summarizes the lattice parameter data calculated from the XRD patterns of a series of Si-MCM-41 materials over the synthesis time ranging from 3 to 47 days, as supplementary information to Figure 2.3:

Table 2.1 Room temperature synthesis of Si-MCM-41:  $a_0$  versus synthesis time

Synthesis time/days	$d_{100}/\text{Å}$	Lattice parameter ( $a_0$ )/ $\text{Å}$
3	38.6	44.6
5	38.1	44.0
10	38.5	44.5
15	38.8	44.8
20	39.6	45.7
30	38.0	43.9
47	36.7	42.4

The lattice parameters have a mean of  $44.3 \text{ Å}$ , with a relative error of 1.6 %. Thus, even though there are signs of a decrease in the unit-cell size after 15-20 days of synthesis, the lattice parameters of these materials over these preparation times are essentially constant. However, after 20 days of synthesis, the lattice parameters do show a gradual decrease. This decrease may be attributed to the prolonged contact between the formed silicate and the basic medium in which it is formed, resulting in the partial solubility of the product, and consequently an increase in the amount of amorphous phase (partial collapse of the porous structure).

The unstirred synthesis of Si-MCM-41 using surfactant templates with different alkyl chain lengths, and mixtures of templates at room temperature over a 5 day period has also been investigated by XRD. Figure 2.4 below summarizes the findings on the effects of the surfactant alkyl chain length:

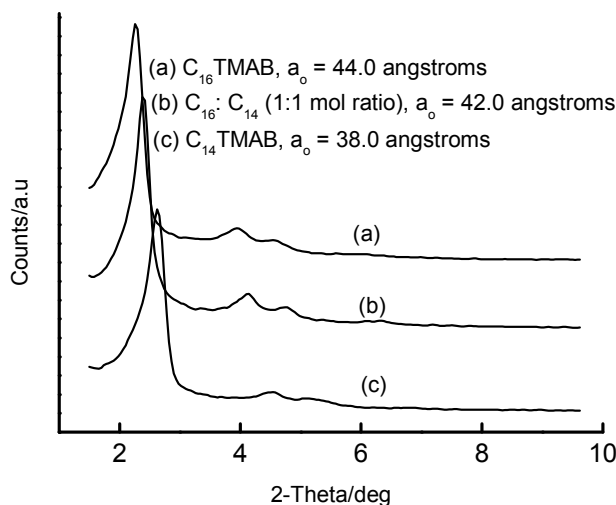


Figure 2.4. XRD patterns of Si-MCM-41 made at RT using templates of different alkyl chain lengths.  ${}^a\text{C}_{14}$  represents tetradecyltrimethylammonium bromide, and  $\text{C}_{16}$  represents cetyltrimethylammonium bromide (a.k.a. CTAB)

The figure above (Fig. 2.4) shows a conspicuous shift in the (100) peak towards the right as the lattice parameters of the materials decrease. The trend shown by the data in the above figure is in accord with literature reports [6, 7] on the effect of the surfactant template alkyl chain length on the pore diameter and lattice parameter of the M41S mesoporous materials. Tetradecyltrimethylammonium bromide (14 C atoms) has a shorter alkyl chain than hexadecyltrimethylammonium bromide (16 C atoms) and therefore the latter results in a material with a larger pore diameter ( $d_{100}$  peak shifts to the left in the XRD pattern). Also, using a 1 : 1 mixture (mole ratio) of the two surfactants as a template and carrying out the synthesis under similar conditions results in a Si-MCM-41 material with pore dimensions intermediate between those of the materials obtained from individual templates. However, the lattice parameter of Si-MCM-41 obtained from mixed surfactant templates is closer to that of the material obtained from the sole usage of a 16 C template. This suggests that the 16 C template plays a more significant role in determining the sizes of the pores. The pores are normally determined by the size of the occluded template after synthesis, and so it can be concluded that most of the 16 C template is occluded

inside the pores of Si-MCM-41 upon their formation, and the smaller 14 C species is either diffusing easily through the bigger pores or mostly taking part in directing the hierarchical ordering of the silicate.

The SiO<sub>2</sub>/CTAB molar ratio of the synthesis gel has also been investigated (using XRD) as a variable influencing the quality and structure of Si-MCM-41 prepared by room temperature synthesis over a 5 day period (see Figure 2.4). Carrying out the syntheses of Si-MCM-41 materials under static (unstirred) conditions using a well-mixed synthesis gel of different silica/surfactant molar ratios, gave rise to mesoporous silica materials with structural properties summarized in Table 2.2 below:

Table 2.2 Effect of gel SiO<sub>2</sub>/CTAB mole ratio on the structure of Si-MCM-41

SiO <sub>2</sub> /CTAB	d <sub>100</sub> /Å	a <sub>0</sub> /Å
1.25	40.9	47.2
2.38	38.1	44.0
3.25	37.9	43.8
5.00	38.9	44.9
8.00	36.5	42.1

This table (Table 2.2) clearly shows the effect of the relative amount of surfactant in the synthesis of mesoporous materials. There is a decrease in the unit cell parameter of Si-MCM-41 as the SiO<sub>2</sub>/CTAB mole ratio of the synthesis gel increases, i.e., a<sub>0</sub> decreases with a decrease in the amount of the surfactant template needed to obtain good quality mesoporous Si-MCM-41. With a gel whose relative composition comprises a larger amount of the surfactant template, the unit cell size, which is related to the pore diameter, is higher than in those containing less amounts of the template. This is suggestive of the pillaring role of the surfactant as it is occluded in the channels after their formation, i.e., increased surfactant content causes increased steric effects and stretching of the pore dimensions. Since a<sub>0</sub> is related to the pore

diameter of the MCM-41 channel system, reduced  $a_0$  implies reduced pore diameters as a consequent. Although Vartuli et al [13] have reported that MCM-41 could be obtained from a synthesis gel with a surfactant to silicon ratio (the reciprocal of the convention used in the above table) of 0.6, the data given in the table above suggests the existence of a range of surfactant/silicon ratios (0.8-0.125) within which Si-MCM-41 materials can be obtained under room temperature synthesis conditions.

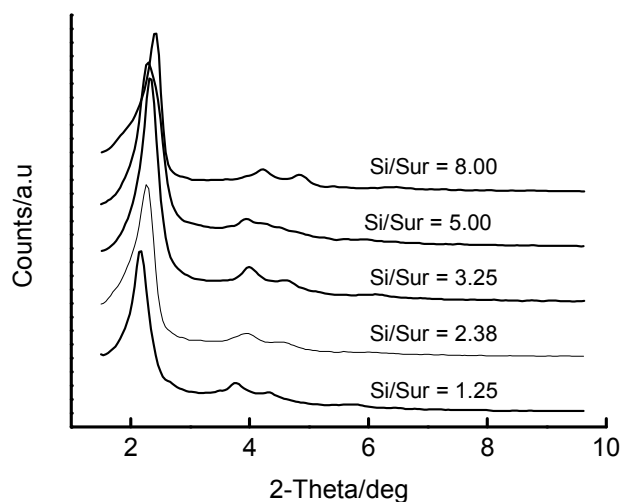


Figure 2.5. The XRD patterns of Si-MCM-41 prepared at RT from gels of varying silicon/surfactant ratios

Indeed, the figure above confirms that all the Si-MCM-41 materials prepared at room temperature over 5 days, with the given range of silicon/surfactant molar ratios, are mesoporous and differ in the degree of long-range order. From this figure, it may be concluded, on the basis of XRD peak intensity and the lattice parameter, that the optimum silicon/surfactant ratio for the preparation of Si-MCM-41 under ambient temperature conditions is  $\sim 3$ .

Another variable investigated in the room temperature synthesis of Si-MCM-41 over 5 days was the water content of the synthesis at a constant pH of 10, reported as (mol  $H_2O$ /mol  $SiO_2$ ). The results of XRD studies on the resulting materials are depicted in

Figure 2.6 below, as a plot of the lattice parameter ( $a_0$ ) versus the  $\text{H}_2\text{O}/\text{SiO}_2$  molar ratio of the synthesis gel:

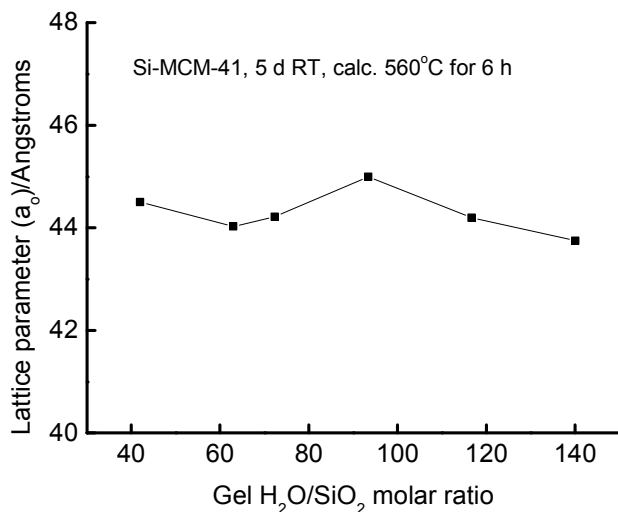


Figure 2.6. Variation of the lattice parameter with synthesis gel  $\text{H}_2\text{O}$  content (RT, 5 days)

Figure 2.6 shows that despite slight deviations, the lattice parameters of the resulting Si-MCM-41 remain essentially constant with a mean of  $44.2 \text{ \AA}$  in the studied range of water content. An important deduction suggested by these data is that for the room temperature synthesis, the quality of the material is insensitive to the amount of water added to the synthesis gel in the  $\text{H}_2\text{O}/\text{SiO}_2$  range of 42 to 140.

In one synthesis, a preformed Si-MCM-41 (which has been calcined at  $560 \text{ }^\circ\text{C}$  for 6 h) was used as a  $\text{SiO}_2$  source in lieu of sodium silicate in a secondary synthesis of Si-MCM-41. The synthesis was carried out at room temperature for 2 days with all the other synthesis variables kept constant. Figure 2.7 shows a comparison of the XRD patterns of the resulting material and its parent:

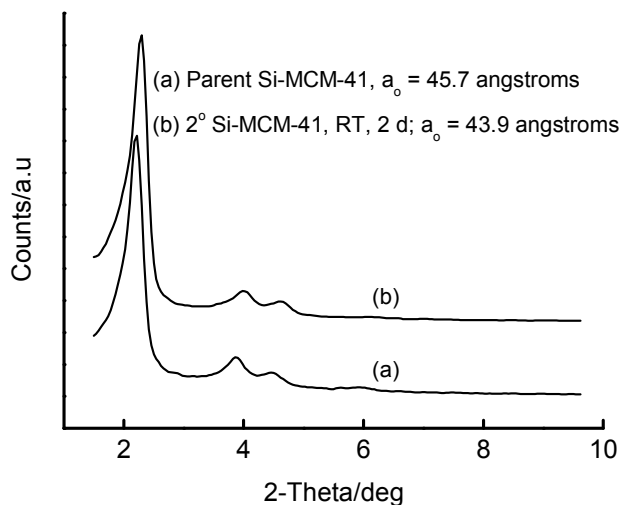


Figure 2.7. XRD patterns of secondary Si-MCM-41: (a) primary Si-MCM-41 (parent), and (b)  $2^\circ$  synthesis at RT for 2 days.

The figure above shows that secondary crystallization of Si-MCM-41 from its siliceous parent at room temperature preserves the mesoporous structure. An observable feature in these XRD patterns is that the (100) peak of the secondary siliceous material is shifted to the right by *ca.*  $1.8 \text{ \AA}$ , relative to the (100) peak of the parent Si-MCM-41. This observation is similar to the one reported by Mokaya et al [18, 19, 27] for the similar synthesis under hydrothermal conditions. These authors attributed this shift to a decrease in pore diameter caused by thickening of the pore walls of this material, a feature that enhances the thermal and hydrothermal stability of these otherwise hydrothermally-unstable materials.

The effect of changing the order of mixing of the synthesis gel precursors by titrating the water-glass solution with a calculated amount of 1 M  $\text{HNO}_3$  solution before mixing and homogenizing the resulting silica species with the surfactant solution, was also studied. Figure 2.8 shows the XRD pattern of the resulting material after room temperature synthesis over a 5 day period.

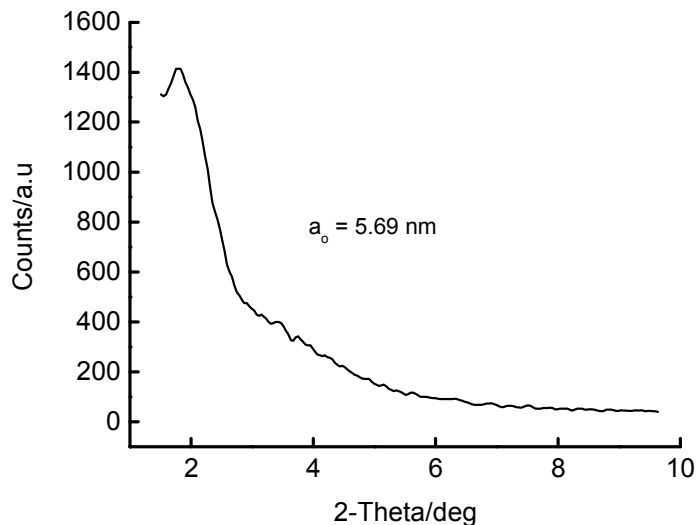


Figure 2.8. XRD pattern of Si-MCM-41 prepared by aging at RT for 5 days, with water glass first titrated with HNO<sub>3</sub> prior adding to CTAB solution. Calcined at 560 °C for 6 h.

As Figure 2.8 shows, carrying out the synthesis at room temperature for 5 days under static (unstirred) conditions gave rise to a less ordered Si-MCM-41 material, as confirmed by an ill-defined XRD pattern with  $a_0 = 56.94 \text{ \AA}$ , and no higher order peaks after calcination at 560 °C for 6 h. The reason for this poor structure may be that titrating the sodium silicate solution with an acid shifts the equilibrium from the anionic silicate to the silanol side, resulting in little or no electrostatic interaction with the cationic surfactant template, which is responsible for directing the structure of the final mesoporous material.

### ***2.3.1.2 Hydrothermal Synthesis***

The successful synthesis of Si-MCM-41 materials at room temperature described in the preceding sections has led us to investigate the synthesis of such materials under conditions reminiscent of the original ones used by the Mobil researchers [6, 7], i.e., hydrothermal conditions at 150 °C for 48 h. In this light, synthesis temperatures of 75, 100 and 120 °C with synthesis gels of pH~10 have been investigated under static

(unstirred) conditions. Figure 2.9 below illustrates the XRD patterns of the resulting calcined siliceous materials:

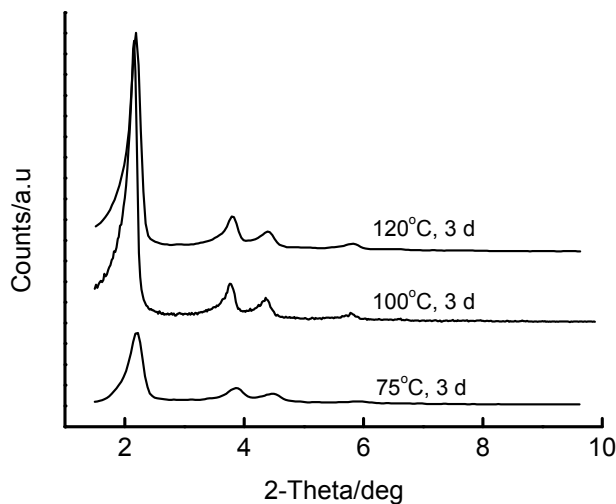


Figure 2.9. XRD patterns of Si-MCM-41 showing the effect of synthesis temperature (3 days synthesis).

The XRD features shown by these materials are in accord with the previous observations in the literature [6, 7], showing the presence of four peaks at low angles and characterizing a hexagonal unit cell. The degree of order in the mesostructure improves with the increase in the synthesis temperature, as marked by the prominence of the (100) peak and the appearance of three higher order peaks with indices (110), (200) and (210). The (100) peak of the material synthesized at 75 °C is not only less intense, but shows a pronounced shift to the right relative to those of materials prepared at 100 and 120 °C. The higher order peaks of this material are also less sharp when compared to the latter two, again suggesting a comparatively inferior order in the channel structure. The appearance of the well-resolved higher order peaks in the above XRD pattern illustrates the long-range order of the channel system. For the materials prepared at 100 and 120 °C respectively, it appears that the former has a more organized mesostructure than the latter, if attention is focused on the position and shapes of the (100), (110), (200) and (210) reflection peaks in the corresponding

XRD patterns. The (100) peak (which is associated with mesoporosity) of the Si-MCM-41 material made at 120 °C, shows a slight shift to the right relative to the 100 °C material and thus suggests a reduction in pore the diameter of his material. Figure 2.10 below provides supplementary data (in the form of lattice parameters) to the information represented by the XRD patterns in the preceding figure.

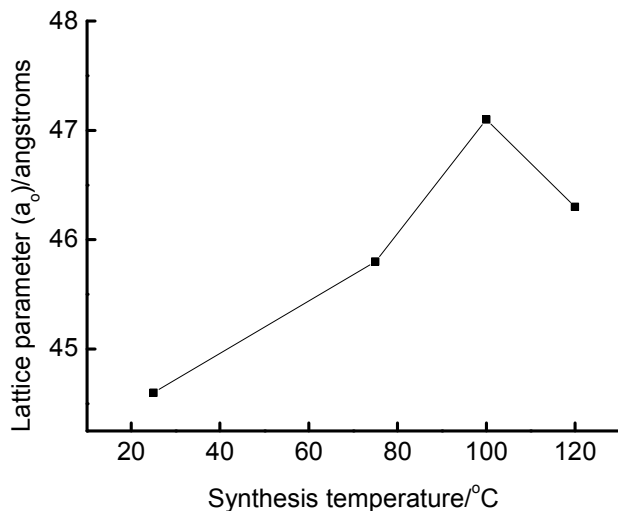


Figure 2.10. A plot of  $a_0$  versus synthesis temperature for Si-MCM-41, 3 days synthesis. Room temperature has been arbitrarily taken as 25 °C.

The above figure shows an initial increase in the lattice parameter with the synthesis temperature up to 100 °C, followed by a decrease when the synthesis is carried out at 120 °C. However, this increase in the lattice parameter is not significant ( $\sim 5.6\%$  increase), with the values being spread around the mean lattice parameter in the interval  $46 \pm 1 \text{ \AA}$ . The improvement in the quality of MCM-41 brought about by increasing the synthesis temperature is only evident from the consideration of the XRD patterns, and is evidenced by the high degree of resolution of the (110) and (200) peaks in the XRD patterns. This reduction in the lattice parameter at 120 °C may signify partial collapse of the pore system due to the instability of the MCM-41-type materials at higher temperatures and possibly a change of phase into either an amorphous phase or into one of the members of the M41S family of zeolites [28, 29].

Interestingly, the reduction in the lattice parameter between the material prepared at 100 °C and that prepared at 120 °C is not significant, i.e., ~ 1.7 % decrease.

The pH of the synthesis gel has also been investigated as a variable to evaluate the quality of the product Si-MCM-41 materials prepared by hydrothermal synthesis. Figure 2.11 below shows the XRD patterns of Si-MCM-41 materials prepared at 100 °C using gels with pH values of 2, 12 and 14:

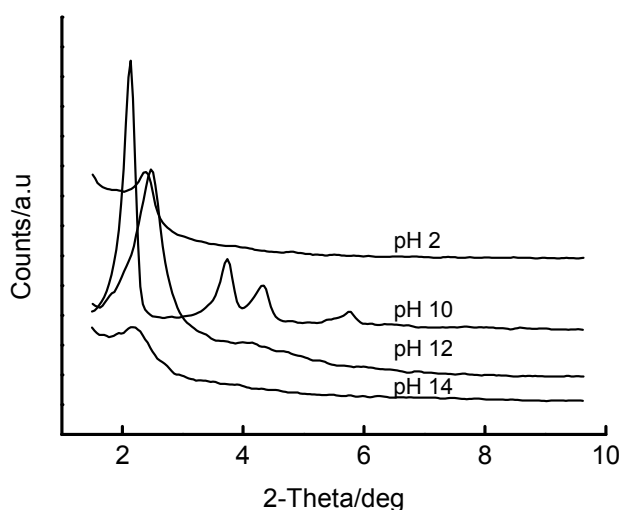


Figure 2.11. XRD patterns of Si-MCM-41 made from gels with different pH values (2 days)

Only one peak indexed as (100) is observed in the XRD patterns of the materials prepared from synthesis gels of pH 2, 12 and 14. In contrast, the material made from a synthesis gel of pH 10 shows excellent mesoporous characteristics, with four peaks at low angles that are indexable on a hexagonal unit cell to (100), (110), (200) and (210). Very low pH values and very high pH values were found to yield a poorly structured mesoporous material, with highly reduced intensities of the (100) peak. The material prepared from a gel of pH 12 shows better mesoporosity than those materials obtained from extremely acidic and extremely basic synthesis gels. The worst porous structure is observed in the material obtained from a synthesis gel with pH 14. This ill-defined porous structure can be attributed to the partial solubility of

silica in extremely alkaline media [2]. It can thus be concluded that extremely low and extremely high pH values of the synthesis gel are detrimental to the quality of the resulting Si-MCM-41 materials. Similar observations have been reported by Wang and Kabe [17], although their XRD patterns were not as well-resolved in the higher order peak region. Therefore, pH 10 has been chosen as the optimum synthesis gel pH for the preparation of Si-MCM-41 and the one-step synthesis of its (Fe, Co)-derivatized analogues. An important point to note in this synthesis is that the pH of the supernatant at the end of the synthesis is always between 11 and 12.

In another synthesis involving control of the pH of the synthesis gel, the pH adjustment was repeated (3 times over a 4 days synthesis period) during the hydrothermal (100 °C) synthesis of Si-MCM-41. This treatment was also found to improve the structural order of the product as deduced from the XRD pattern shown in Figure 2.12 below:

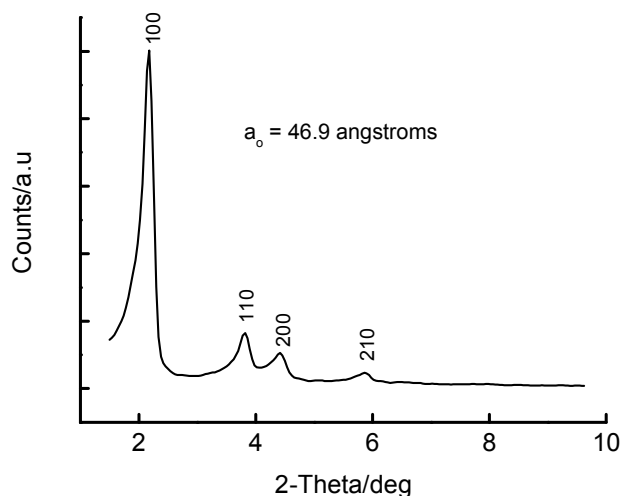


Figure 2.12. The XRD pattern of Si-MCM-41 prepared by intermediate pH adjustment

Even though the high-pressure crystallization process was interrupted at intervals to bring the gel pH to 10 by addition of an acid solution, the resulting material shows a high degree of order. Previous reports [23, 26, 30] have recommended this method as

a way of improving both the structural order and the hydrothermal stability of pure silica MCM-41. The calculated lattice parameter ( $a_0$ ) shows that this material is no better than the one in which the pH was adjusted only before the hydrothermal synthesis using the same synthesis recipe. Therefore, for the rest of the syntheses reported in this work, only the initial pH adjustment was performed prior to hydrothermal synthesis of Si-MCM-41.

The crystallization time during the synthesis of Si-MCM-41 has been investigated as a synthesis variable in order to optimize the time needed for good quality materials. The XRD patterns of the Si-MCM-41 materials prepared from a synthesis gel with the same composition as that used for room temperature in the preceding sections, but with the synthesis carried out at 100 °C for different time periods, are shown in the Figures 2.13 below. Figure 2.13 (a) shows the full  $2\theta$  range for MCM-41, whereas Figure 2.13 (b) depicts the higher-angle region ( $3^\circ \leq 2\theta \leq 10^\circ$ ) of the same material in order to study the effect of hydrothermal synthesis on the long-range order of these materials.

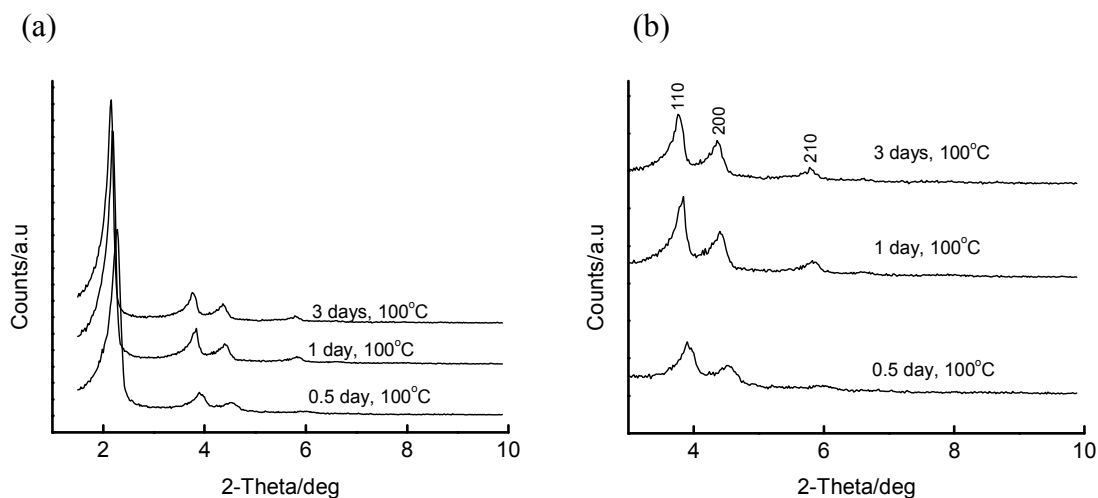


Figure 2.13. XRD patterns of calcined Si-MCM-41 prepared at 100 °C for 12-72 h: (a)  $1^\circ \leq 2\theta \leq 10^\circ$ , and (b)  $3^\circ \leq 2\theta \leq 10^\circ$  (higher order region).

The observations in the above figure can be summarized by a plot of the lattice parameter versus the synthesis time, as shown in Figure 2.14 below:

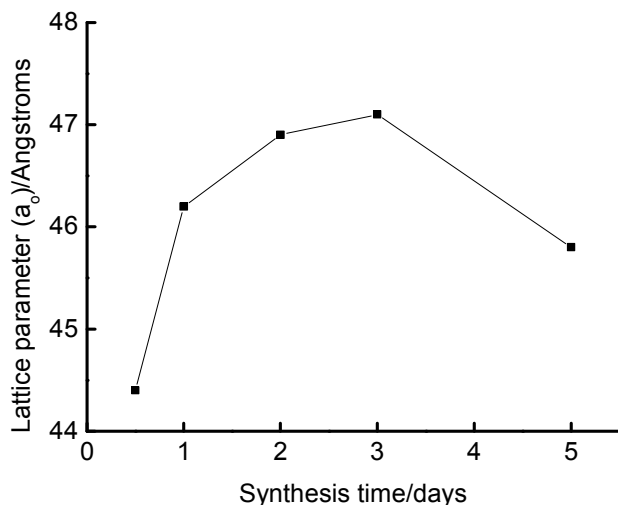


Figure 2.14. Variation of  $a_0$  with synthesis time at 100 °C for Si-MCM-41

The above figure shows that the unit cell parameter,  $a_0$ , increases with synthesis time and attains a maximum after 3 days. It then decreases as the synthesis time is extended to 5 days. This observation suggests that the oligomerization and condensation of the silicate species is only complete between 2 and 3 days of hydrothermal synthesis, suggesting the existence of an optimum synthesis time. The observed decrease in the lattice parameter (structural pore contraction) of the Si-MCM-41 material prepared over 5 days can suggest that the material becomes amorphous with the extended synthesis. The high BET surface area of this latter material ( $1197 \text{ m}^2 \cdot \text{g}^{-1}$ ) may also be a good sign that an amorphous material is advanced at this synthesis time. This amorphization can partially result from the fact that the final pH of the reaction mixture after synthesis is  $\sim 12$ , which may tend to promote the dissolution of the product Si-MCM-41.

The superiority of the hydrothermal synthesis (100 °C) over room temperature synthesis in the preparation of Si-MCM-41 is demonstrated in Figures 2.15 (a) and (b), with different synthesis times:

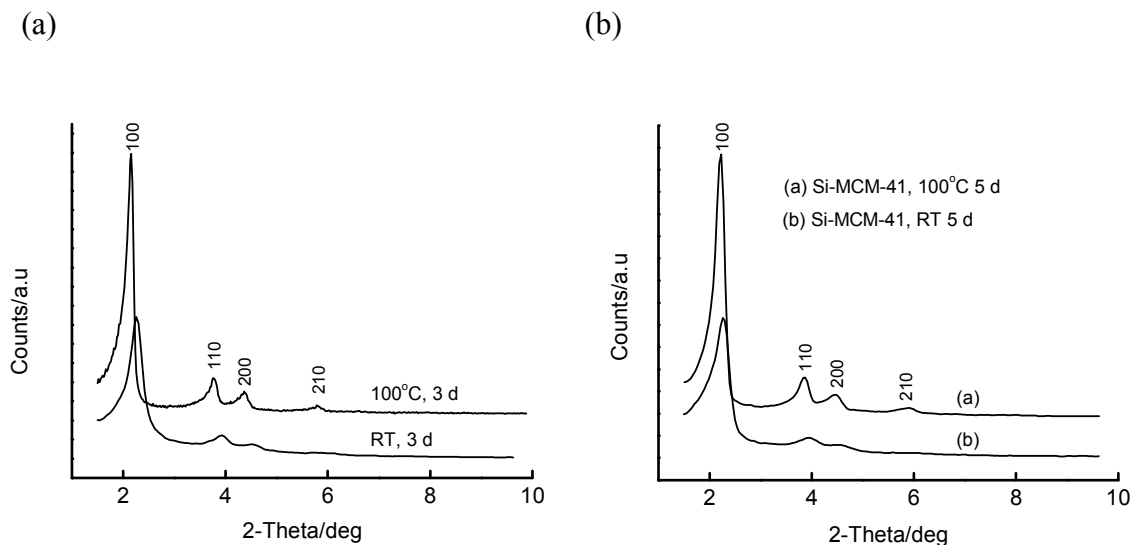


Figure 2.15. XRD patterns of Si-MCM-41, RT v/s 100 °C synthesis: (a) 3 days, (b) 5 days

As expected (see section 2.3.1.1), the water content of the synthesis gel under hydrothermal conditions (100 °C) for the synthesis of Si-MCM-41 over 2 days has shifting effects on the structural properties of the resulting materials. Figure 2.16 illustrates the trend in lattice parameters.

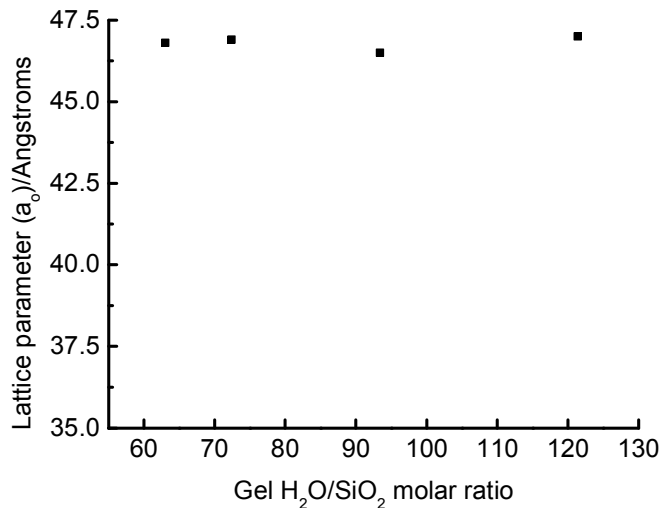


Figure 2.16. A plot of lattice parameter versus gel H<sub>2</sub>O/SiO<sub>2</sub> molar ratio (Si-MCM-41, 100 °C, 2 days)

In a further synthesis of Si-MCM-41, the distilled water solvent was replaced by a pH 10 buffer solution, with all the other gel components fixed and the synthesis carried out at 100 °C for 2 days. XRD analysis of the resulting material after the post-synthesis processing gave results depicted in the following figure:

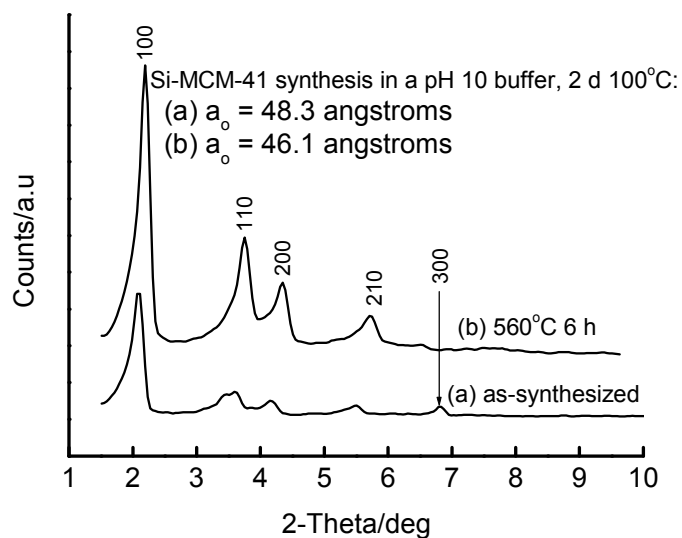


Figure 2.17. XRD patterns of Si-MCM-41 prepared in a pH 10 buffer solution

A notable feature in the above XRD patterns is the appearance of a (300) peak in the as-synthesized (surfactant-containing) Si-MCM-41 material, which seems to be absent in the calcined sample. However, the enhanced intensities of the diffraction peaks observed in the pattern of the calcined material suggest increased pore ordering than in the uncalcined sample. The absence of the (300) peak in this apparently highly ordered material may relate to an effect of preferred orientation. It is also worth noting that upon calcination of the as-synthesized material, the diffraction peaks are shifted to the right as the pore diameter contracts. This pore contraction manifests itself through the decrease in the lattice parameter from 48.3 Å to 46.1 Å upon calcination at 560 °C for 6 h (i.e. 4.6 % lattice contraction). It can thus be concluded that the materials prepared via this method are reasonably thermally stable, as lattice contractions as much as 25 % upon calcination have been observed in other studies [31-34].

Another synthesis variable studied in this work was the possibility of doubling the synthesis gel composition to prepare larger batches of material. Si-MCM-41 was then synthesized at 100 °C for 48 h using a gel composed of twice the molar concentration given in the experimental section above, in order to obtain a larger quantity of the product. Figure 2.18 shows the XRD pattern of the resulting material after calcination at 560 °C for 6 h.

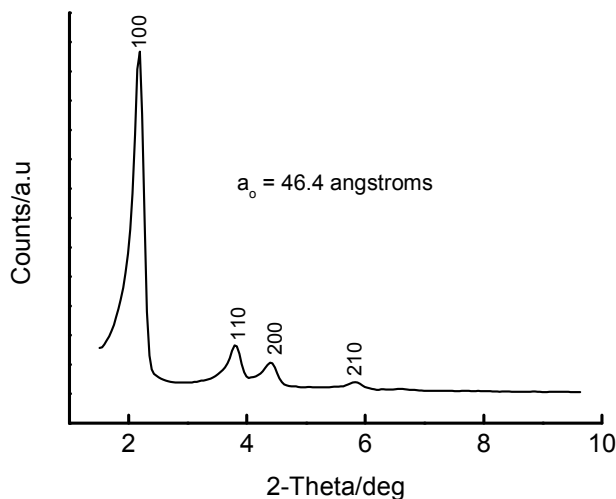


Figure 2.18. XRD pattern of Si-MCM-41 prepared by doubling the gel composition

Therefore, larger batch sizes of Si-MCM-41 can be prepared with maximal retention of the structural features known for these materials.

The nature of the mineral acid used for adjusting the pH of the synthesis gel to 10 was also investigated for the possible effect on the structural properties of the resulting Si-MCM-41. Figure 2.19 shows the effect of the identity of the mineral acid used for pH adjustment to 10 in the synthesis of Si-MCM-41 under hydrothermal conditions (100 °C for 2 days). The materials were subsequently calcined at 560 °C for 6 h.

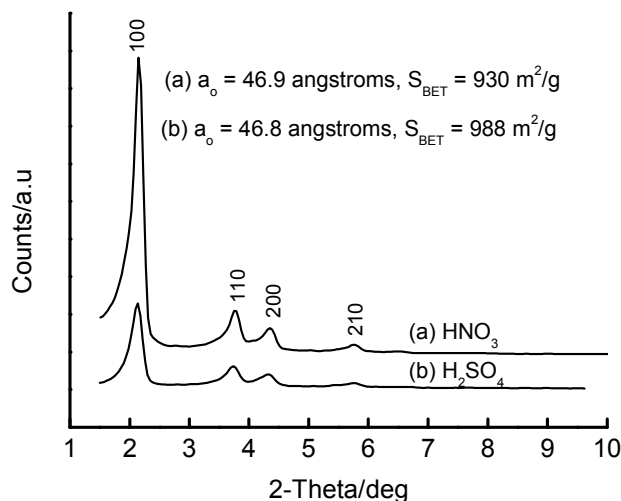


Figure 2.19. XRD patterns of Si-MCM-41 prepared by using different acids

Figure 2.19 shows that the peak positions for the two Si-MCM-41 materials above are not significantly distinct, as can also be seen from the calculated lattice parameters. Observable though, is the improved intensity of the Bragg peaks for the material whose gel pH was adjusted using HNO<sub>3</sub> as compared to that using H<sub>2</sub>SO<sub>4</sub>. This may suggest a high structural order in the material made with HNO<sub>3</sub>, implying a relatively more amorphous phase content in the material prepared by pH adjustment with H<sub>2</sub>SO<sub>4</sub>. The surface area data (included on the figure for substantiation purposes) is higher for the Si-MCM-41 synthesized using H<sub>2</sub>SO<sub>4</sub> than its HNO<sub>3</sub> counterpart. The BET data partially supports the observation from the XRD patterns that there is more amorphous material in Si-MCM-41 where sulphuric acid was used to adjust the pH of the synthesis gel, as amorphous materials are expected to have higher surface areas than crystalline ones.

Figure 2.20 shows the effect of calcining the as-synthesized (surfactant-containing) Si-MCM-41 on the XRD patterns of these materials.

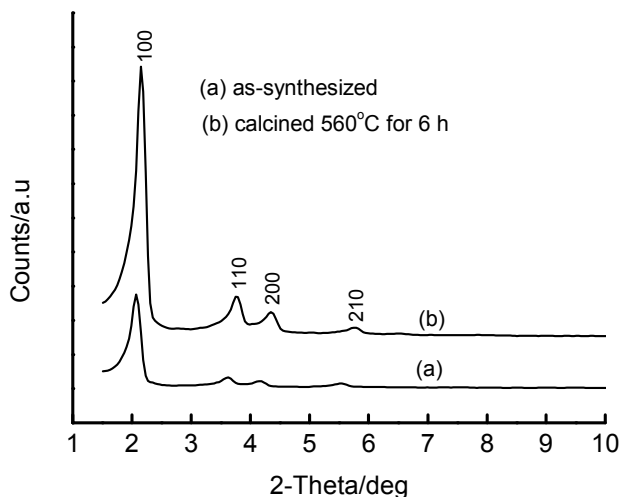


Figure 2.20. XRD patterns of Si-MCM-41 synthesized at 100 °C for 2 days.

As can be seen from Figure 2.20, the uncalcined Si-MCM-41 material has the  $d_{100}$  peak maximum to the left of the calcined material, implying a larger  $a_0$  value in the former material. However, the intensity of the  $d_{100}$  peak in the as-synthesized siliceous material and its higher order peaks is lower than the intensity of the corresponding peaks in the calcined material. The lower intensity can be attributed to the possibility of destructive interference from the diffraction planes associated with the occluded template. Upon removal of the template, diffraction from the silica planes lead to enhanced constructive interference and consequently more intense peaks. This treatment is always accompanied by a reduction in the unit cell parameter as the occluded template acts like a pillar and holds the pore apart.

The nature of the silica source in the synthesis of Si-MCM-41 under hydrothermal conditions (100 °C for 2 days) has also been investigated as a variable determining the quality of the final material. The quality of the resulting mesoporous phases was assessed by X-ray powder diffraction, and the results are depicted in Figure 2.21 below:

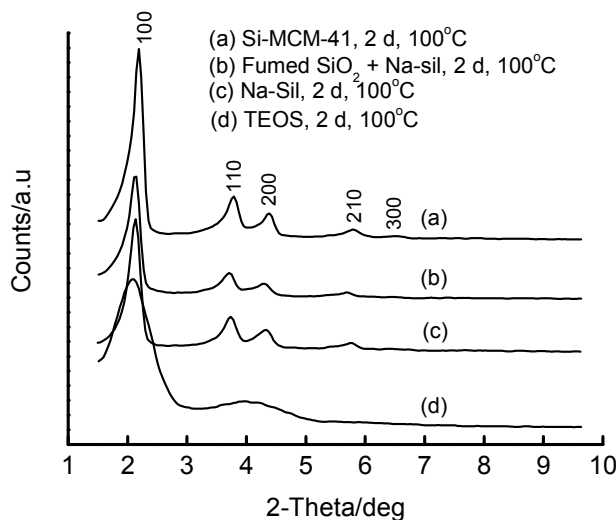


Figure 2.21. XRD patterns of Si-MCM-41, showing the effect of the silica precursor

Figure 2.21 above shows that the quality of the mesoporous silica MCM-41 depends on the type of silica source used in the synthesis recipe. Although the four materials whose XRD patterns are given above are mesoporous (all have the  $d_{100}$  Bragg peak), the material derived from tetraethyl orthosilicate (TEOS) is found to lack long-range order. In contrast, the Si-MCM-41 materials prepared using water-glass (sodium silicate), a mixture of water-glass and fumed silica, as well as calcined Si-MCM-41 (primary siliceous MCM-41) all show a high degree of order in their channel system. Remarkably, the material prepared from calcined Si-MCM-41 as a silica source shows the most ordered structure, with the appearance of an additional peak designated as (300) in the XRD patterns. This extended order in secondary Si-MCM-41 can be attributed to the fact that in this synthesis, an already ordered material was used as a starting material. The broad (100) peak in the XRD pattern of the Si-MCM-41 as compared to the other samples may be attributed to the polarity of TEOS, which is not well-suited for electrostatic interaction with the cationic surfactant template used in the synthesis (i.e., the cetyltrimethylammonium cation). In the compound silica source, with a mixture of water glass and fumed silica, the water glass may be regarded as a primary condensation reactant because of charge matching between the

silicate and the cationic surfactant, and this may induce further condensation of fumed silica.

Figure 2.22 below illustrates the effect of calcination temperature on the structural properties of secondary Si-MCM-41 (prepared using Si-MCM-41 as a silica source, at 100 °C over 2 days). The duration of the calcination at a particular temperature was 6 h:

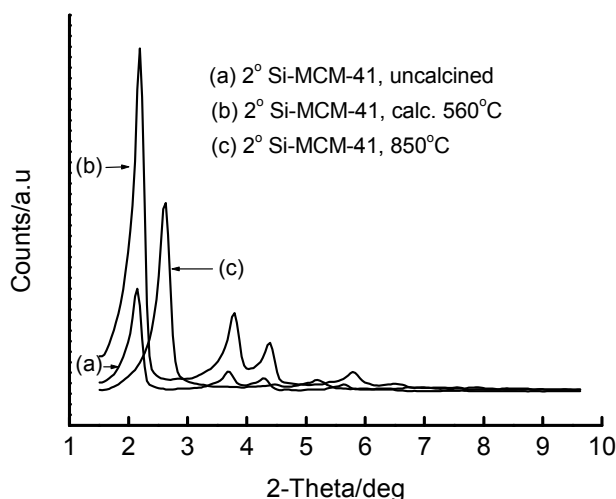


Figure 2.22. XRD patterns of secondary Si-MCM-41: Effect of calcination temperature

The figure above shows that there is an improvement in the mesostructure of Si-MCM-41 upon calcination at 560 °C. The  $d_{100}$  diffraction peak shifts slightly to the right as a result of combustion of the surfactant template that is occluded in the pores of the as-synthesized material. This decomposition of the template causes partial shrinkage of the pore as the silicate framework relaxes to an equilibrium position when the prop (occluded surfactant) burns off. The higher calcination temperature (850 °C) is accompanied by a comparatively higher reduction in the size of the pores (significant shift of the (100) peak to the right) and also the loss of long-range structural order. Interestingly, most of the mesostructure is still retained after calcination at 850 °C.

Secondary synthesis of Si-MCM-41 was also performed at 100 °C for a longer time (96 hours) using calcined Si-MCM-41 as a SiO<sub>2</sub> source instead of water-glass, and XRD analysis gave the results summarized in Table 2.3.

Table 2.3 XRD properties of *sec*-Si-MCM-41 (100 °C, 4 days)

Sample	$d_{100}/\text{Å}$	$a_0/\text{Å}$
Parent Si-MCM-41	40.6788	47.0
<i>sec</i> -As-synthesized	40.4922	46.8
<i>sec</i> -Calcined 560 °C, 6 h	38.7165	44.7

Calcination is always accompanied by a reduction in the lattice parameter in both primary and secondary synthesis. The  $a_0$  in the *sec*-Si-MCM-41 is lower than that of the parent, a property which has been attributed to increased crystallinity and enhanced hydrothermal stability due to an increase in the pore wall thickness of these materials upon secondary synthesis [18, 19, 27]. The *sec*-synthesized material under the same conditions but with the synthesis carried out over 2 days was found to undergo a decrease in  $a_0$  value from 48.3 to 46.1 Å (a 4.6 % reduction) upon calcination at 560 °C for 6 hours, whereas that prepared over 4 days decreased from 47.0 to 44.7 Å (a 4.9 % reduction). Therefore, the reduction in the lattice parameter of Si-MCM-41 upon secondary synthesis seems to be insensitive to the synthesis time (or extent of synthesis) within a tolerable experimental error.

The extent of carrying out the secondary synthesis of Si-MCM-41 under hydrothermal conditions has also been investigated. The degree of long-range order in the resulting materials was studied by X-ray powder diffraction, and the patterns are shown in Figures 2.23 (a) and (b) below:

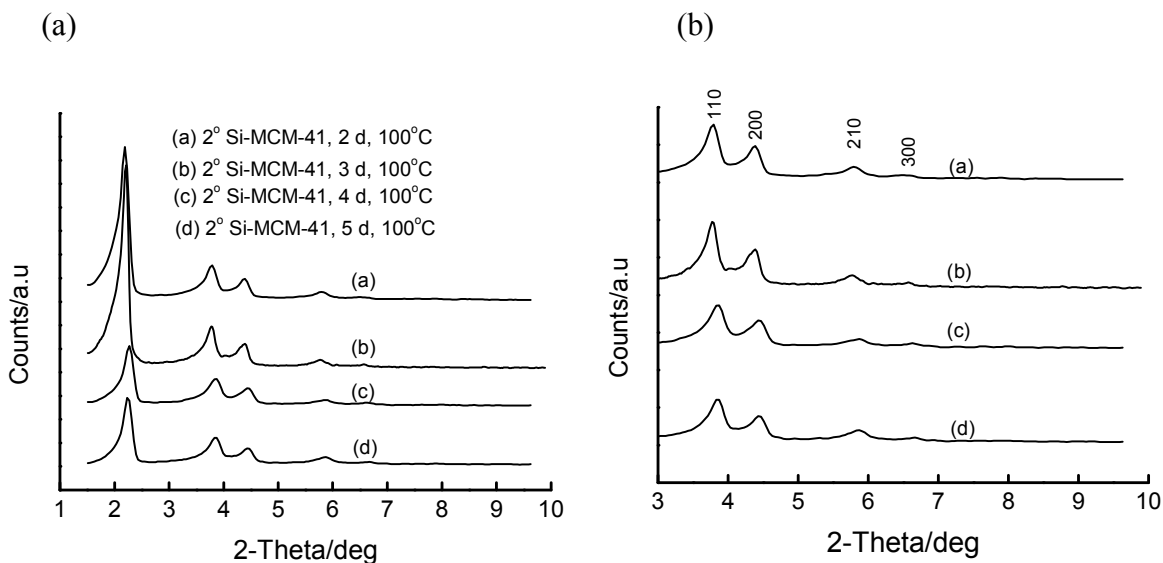


Figure 2.23 . The XRD patterns of secondary Si-MCM-41: Effect of synthesis time, (a) full range, and (b)  $3^\circ \leq 2\theta \leq 10^\circ$

The Figures 2.23 (a) and 2.23 (b) above show the dependence of structural order of secondary Si-MCM-41 on the hydrothermal crystallization time. There is an apparent small shift in the  $d_{100}$  peak of these materials as the crystallization time increases. All these materials show a small/weak  $d_{300}$  peak in their XRD patterns (Figure 2.23 (b)). An important observation in the above figures is that all the diffraction peaks in the secondary Si-MCM-41 prepared over 3 days are more intense and sharper than those of the other materials reported on this figure. The trend in the figure suggests an improvement in the long-range order on moving from 2 days to 3 days (conspicuous peak narrowing), followed by a gradual but minimal loss in long-range order on progressing to 4 and 5 days of hydrothermal synthesis of *sec*-Si-MCM-41.

In one other synthesis, part of the synthesis gel prepared by pre-hydrolysing the sodium silicate solution with 1 M  $\text{HNO}_3$  solution before mixing with the template solution was subjected to a high temperature treatment at  $97^\circ\text{C}$  for 45 minutes. After processing and final calcination, the resulting Si-MCM-41 material showed the XRD properties depicted in the Figure 2.24 below:

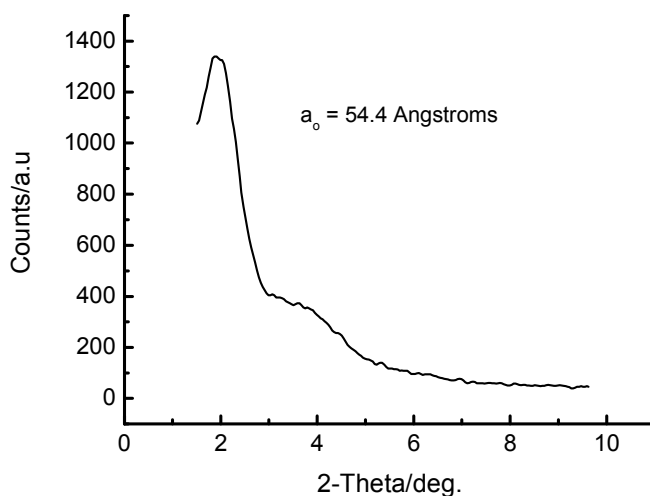


Figure 2.24. XRD pattern of Si-MCM-41 prepared by heating the synthesis gel (97 °C for 45 min) made with pre-hydrolysis of water-glass with HNO<sub>3</sub> before adding to CTAB solution. Calcined at 560 °C for 6 h.

The XRD pattern above shows that the resulting Si-MCM-41 material begins to be ordered (marked by the appearance of a broad feature at about 4 °2θ, signifying the evolution of higher order peaks) upon high temperature treatment, even if the duration of the treatment was as short as 45 minutes. By comparison with the XRD pattern of the material made from the other half of the synthesis gel, but with the synthesis carried out at room temperature for 5 days (Figure 2.8), the heated synthesis produces a relatively more ordered product (with  $d_{100} = 47.0782$  and  $a_0 = 54.36 \text{ \AA}$ ). It can therefore be concluded that silicate crystallization is faster with heating than with room temperature treatment. In previous studies [10], samples with only one distinct reflection have also been found to contain substantial amounts of MCM-41. Note also the similarity of the XRD pattern of this material to that derived from TEOS (Figure 2.21 (d)), signifying the importance of the type of interaction between the SiO<sub>2</sub> precursor and CTA<sup>+</sup> ion. In the present case, titration of water-glass with HNO<sub>3</sub> generates terminal silanols, which interacts with CTAB less efficiently than the Si-O<sup>-</sup> group in water-glass.

Representative XRD patterns of Si-MCM-41 materials prepared under magnetic stirring at 80 °C for 6 h are shown in *appendix A.1*. These materials were prepared using a compound silica source, (water-glass + TEOS). The ratio  $R_{\text{SiO}_2}$ , defined as mol of  $\text{SiO}_2$  in TEOS divided by mol of  $\text{SiO}_2$  in water-glass, was found to affect the lattice dimension, as can be deduced from the shapes and the widths of the (100) reflection peak. The XRD patterns suggest that the quality of the resulting Si-MCM-41 increases as the water-glass content of the synthesis gel increases, with  $R_{\text{SiO}_2} = 1.48$  giving the best results in the series. This observation may further suggest that water-glass is the primary polymerizing species, and induces further condensation of the TEOS.

### 2.3.1.3 Al-Si-MCM-41 Studies

The incorporation of Al during MCM-41 synthesis was also investigated in order to provide a comparison regarding the structure of the final material. This was achieved by the addition of the Al precursor ( $\text{Al}(\text{NO}_3)_3 \cdot 9\text{H}_2\text{O}$ ) at various stages of the synthesis gel preparation, prior to hydrothermal treatment. Al-containing MCM-41 materials were also prepared by incipient wetness impregnation (IWI) of the siliceous parent using aqueous and non-aqueous solvents. XRD studies showed that both types of Al-containing mesoporous materials (those obtained by 1-pot synthesis and those by IWI) were highly ordered, with exactly the same features except for peak positions. Figure 2.25 below shows the XRD patterns of MCM-41 materials (Si/Al = 30) prepared by changing the order of addition of the Al precursor and also introducing an aging period prior to hydrothermal synthesis:

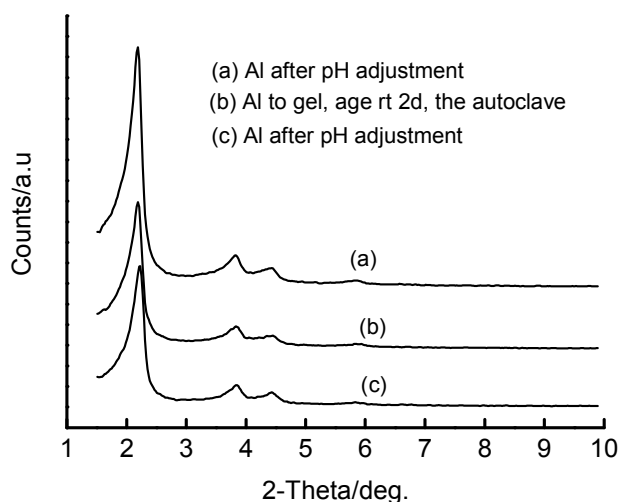


Figure 2.25. XRD patterns of (Al,Si)-MCM-41 (Si/Al = 30) prepared at 100°C for 48 h: (a) Al source added to the gel after pH adjustment, (b) Al source added to the gel before pH adjustment, followed by 2 days aging prior to synthesis, and (c) Al source added to the gel before pH adjustment

The figure above reveals that the point of addition of the Al precursor does not have a pronounced effect on the structural integrity of the final MCM-41 material. All the materials exhibit XRD patterns with four Bragg peaks, which are characteristic of good quality MCM-41. Adding the Al precursor before pH adjustment with an acid solution causes a slight shift of the (100) peak to the right, and this is more apparent in the sample synthesized without prior aging of the synthesis gel. This observation may suggest the incorporation of Al into the silicate framework when the Al precursor is added before the hydrolyzing agent (i.e., the acid), and that when the addition is done after pH adjustment, the Al exists as extraframework species.

Solvent effects were also investigated in the introduction of the Al species into Si-MCM-41 by incipient wetness impregnation. Figure 2.26 shows the XRD patterns of the calcined MCM-41 materials (Si/Al = 22) prepared via IWI using various solvents.

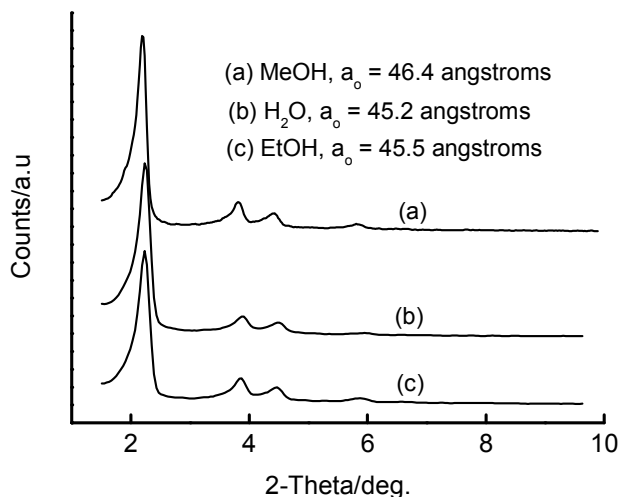


Figure 2.26. XRD patterns of (Al,Si)-MCM-41 (Si/Al = 22) prepared by IWI of Si-MCM-41. (a) methanol as solvent, (b) water as solvent, and (c) ethanol as solvent. IWI abbreviates incipient wetness impregnation.

The above figure shows that the resulting materials are mesoporous and highly ordered as marked by the appearance of well-resolved higher order peaks in addition to the (100). However, slight shifts to the right are observed in the XRD patterns of the Al-containing materials where water and ethyl alcohol were used as solvents, as compared to that made with methanol as a solvent. This may be attributed to the higher temperatures necessary to evaporate the former two solvents (boiling points for water and ethanol are 100 °C and 80 °C, respectively, as compared to 64.7 °C for methanol), which may cause partial collapse of the pores.

A comparison of the structural integrities of the MCM-41 (Si/Al = 22) materials prepared by direct hydrothermal synthesis and by incipient wetness impregnation, (IWI), of the pure silica parent is depicted in Figure 2.27 below:

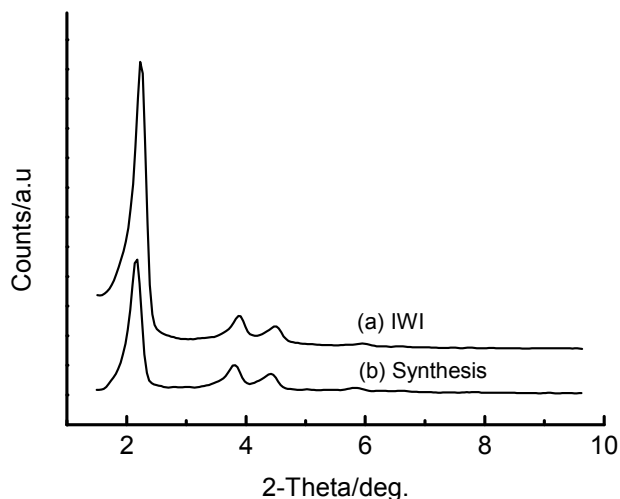


Figure 2.27. XRD patterns of (Al,Si)-MCM-41 (Si/Al = 22) by different synthesis routes

It can be seen from the above figure that these materials are similar, except for the intensities and the width of the peaks. Both these features are prominent in the material made through incipient wetness impregnation, which has the advantage of starting with an already ordered material when aluminium is introduced.

### 2.3.2 BET surface area measurements

#### 2.3.2.1 Room Temperature Synthesized Si-MCM-41 Materials

BET studies have been made on some of the materials synthesized at room temperature in this thesis. The principal aim of carrying out the room temperature was to screen and optimize the working parameters for preparing good quality Si-MCM-41 under hydrothermal conditions. Thus, the results of room temperature synthesized materials serve as benchmarks for the siliceous materials prepared at higher temperatures.

The effect of the synthesis gel water content (in the synthesis of Si-MCM-41 under the same conditions of room temperature synthesis over a 5 days period) on the surface area of the final calcined (560 °C, 6 h) materials was investigated. Figure 2.28 shows the trend in the results obtained in the measurement of the specific surface area.

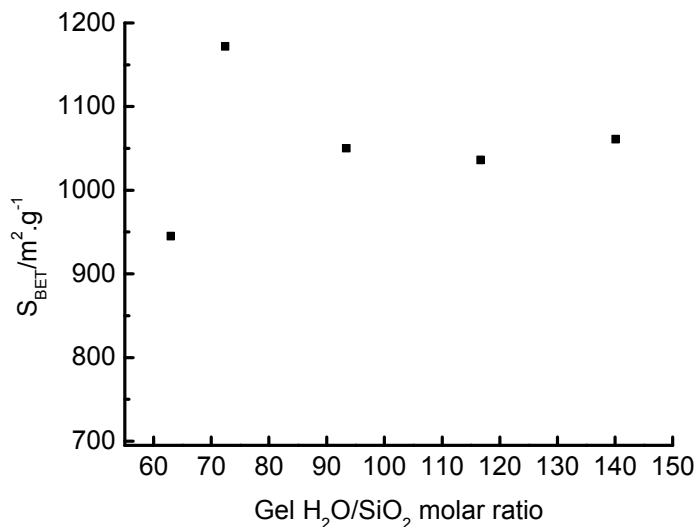


Figure 2.28. Variation of the BET surface area of Si-MCM-41 with gel water content (RT, 5 days)

From the results in the above figure, it is evident that all but one of the siliceous materials prepared at ambient temperature have BET surface areas in excess of 1100 m<sup>2</sup>/g. This observation is supportive of the XRD results plotted in Figure 2.6 and is suggestive of mesoporosity. Although there is an initial increase in S<sub>BET</sub>, it can be seen from the figure that the specific surface area of Si-MCM-41 seems to be insensitive to the amount of water in the gel for the ratio  $93.4 \leq \text{H}_2\text{O}/\text{SiO}_2 \leq 140.1$ . This property was then exploited in the synthesis of transition metal-containing variants of MCM-41 (Chapter 3) via a one pot synthesis, where higher amounts of water were necessary to form a reasonable gel (because the highly charged cationic metal ions have an ordering effect on the water, making their aqueous solutions acidic).

However, carrying out the room temperature synthesis of Si-MCM-41 for 5 days, followed by calcining the resulting material at a slightly lower temperature of 500 °C for 12 hours (with a 1 °C/min ramping rate), produced a material with extremely high surface area of 1344 m<sup>2</sup>.g<sup>-1</sup>.

### 2.3.2.2 Hydrothermally-prepared Si-MCM-41 Materials

The specific surface area of Si-MCM-41 has been studied as a function of the synthesis temperature over a 3 day period, under unstirred conditions. Upon calcination of the as-synthesized materials to remove the occluded surfactant template, the resulting materials showed high surface areas. Table 2.4 below shows the trend of the surface area with synthesis temperature (with an error bar of about 10 %):

Table 2.4 S<sub>BET</sub> versus crystallization temperature (3 days synthesis) for Si-MCM-41

Synthesis temperature/°C	d <sub>100</sub> /Å	Lattice parameter (a <sub>0</sub> )/ Å	S <sub>BET</sub> /m <sup>2</sup> .g <sup>-1</sup>
25 <sup>a</sup>	38.6	44.6	945
75	39.7	45.8	-
100	40.8	47.1	1009
120	40.1	46.3	997

<sup>a</sup>Room temperature has been arbitrarily taken as 25 °C

The data in the above table demonstrate that the surface areas of Si-MCM-41 reported here do not show an obvious trend although suggestive of an increase followed by a decrease, and as such implying the existence of an optimum synthesis temperature for maximum surface area and pore size (related to a<sub>0</sub> = 47.1 Å). The above data, in conjunction with XRD data, also suggest that the siliceous material prepared at room temperature is slightly less ordered than the ones prepared at higher temperatures. In

the XRD pattern of the material prepared at room temperature, there is poor resolution of the peaks above  $2\theta = 2.2^\circ$ , while there is improved resolution in high temperature-synthesized materials. Although there seems not to be an obvious trend in surface area in this temperature range, it can be concluded that the products are mesoporous since their  $S_{\text{BET}} \approx 1000 \text{ m}^2 \cdot \text{g}^{-1}$ . Thus  $100^\circ\text{C}$  was chosen as the optimum temperature for the synthesis of good quality pure silica MCM-41 in this thesis.

The BET surface area of the Si-MCM-41 materials was also studied as a function of the synthesis time for materials prepared at  $100^\circ\text{C}$ . Figure 2.29 below shows the observed trend:

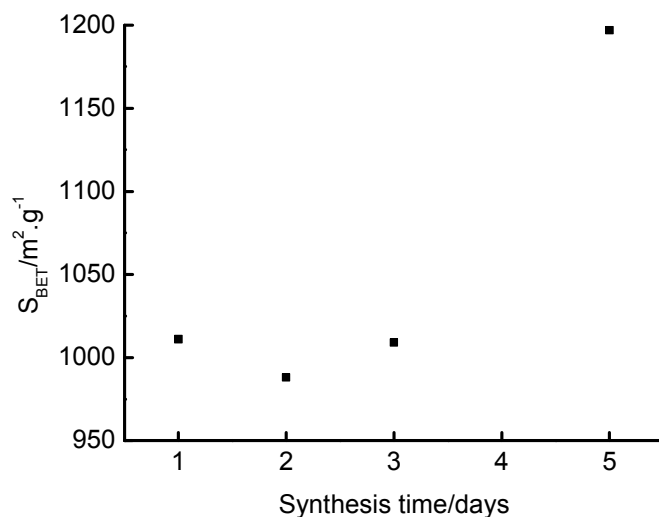


Figure 2.29. Variation of the BET surface area with synthesis time for Si-MCM-41 ( $100^\circ\text{C}$ )

Figure 2.29 shows that the  $S_{\text{BET}}$  remains constant within an experimental error between 1 and 3 days of synthesis and then shoots up steeply beyond this time. This observation can be associated with amorphization of the material on prolonged contact with the alkaline mother liquor, as supported by the partial collapse of the porous structure that manifested itself by the decrease in lattice parameter of this material observed in Figure 2.14. The TEM micrograph of this material also show an amorphous region coexisting with the highly ordered phase (Figure 2.30).

The effect of the water content of the synthesis gel on the BET surface areas of the siliceous products from hydrothermal synthesis (100 °C 2 d) has been investigated for two representative compositions, H<sub>2</sub>O/SiO<sub>2</sub> ratios 63 and 93.4. These ratios were chosen on the basis of the trend observed in the room temperature-synthesized materials, where the ratio 93.4 could be regarded as the ratio necessary for the attainment of the optimum specific surface area. The measured specific surface area was found to be enhanced at the gel water content H<sub>2</sub>O/SiO<sub>2</sub> = 93.4, with a value of 993 m<sup>2</sup>.g<sup>-1</sup>, whereas the value of H<sub>2</sub>O/SiO<sub>2</sub> = 63 gave the BET surface area of 988 m<sup>2</sup>.g<sup>-1</sup>. Interestingly, the lattice parameter remains essentially constant (*appendix A.2*) as the water content is varied. This observation supports the findings of the room temperature synthesis seen above (Figure 2.6). However, at a constant water content of H<sub>2</sub>O/SiO<sub>2</sub> = 72.4 and hydrothermal synthesis at 100 °C, the Si-MCM-41 material prepared over 2 days and that over 5 days had surface areas of 882 and 897 m<sup>2</sup>. g<sup>-1</sup> respectively. It is worth noting that the BET surface area of the secondary Si-MCM-41 is lower compared to those obtained for the primary Si-MCM-41, regardless of the differences in the water contents in the initial synthesis gels. Since the XRD has confirmed little or no significant contribution of the amount of water in the synthesis gel on the product, it can be inferred that the reduced BET surface area observed for the secondary Si-MCM-41 is due to the crystalline nature of its pore walls [19], since the primary Si-MCM-41 consists mainly of amorphous pore walls. Amorphous materials normally have higher specific surface areas [2].

Since a synthesis gel pH of 10 has been found to result in pure silica MCM-41 materials with excellent XRD patterns, two mineral acids were compared as pH adjusting media. Si-MCM-41 materials were prepared at 100 °C using both HNO<sub>3</sub> and H<sub>2</sub>SO<sub>4</sub> to bring the pH of the highly basic (alkaline) sodium silicate gel to 10. Table 2.5 below shows the results of BET surface area measurements on the resulting materials:

Table 2.5 Si-MCM-41 properties: Effect of mineral acid identity

Acid (1 M solution)	Lattice Parameter/Å	S <sub>BET</sub> /m <sup>2</sup> ·g <sup>-1</sup>
HNO <sub>3</sub>	46.9	930
H <sub>2</sub> SO <sub>4</sub>	46.8	988

Although the lattice parameters (given in Table 2.5) of the resulting two materials are similar, the BET surface area data shows a higher value for the material whose pH was adjusted using H<sub>2</sub>SO<sub>4</sub>. It is not clear whether the difference stems from the nature of the anion part of the acid (NO<sub>3</sub><sup>-</sup> versus SO<sub>4</sub><sup>2-</sup>) or from the proticity of the acid used (monoprotic versus diprotic acid). The similarity in the lattice parameters implies that the two materials have the same structural integrity.

The addition of components in the templating solution with the aim of influencing the micelle size has also been studied. A copolymer of methyl vinyl ether and maleic anhydride, and sodium potassium tartrate, were investigated as potential micelle expanders. The effect of including these additives in the synthesis gel during the hydrothermal synthesis, at 100 °C, of pure silica MCM-41 over 48 h from the gel of pH 10 is shown in Table 2.6 (*next page*). Inclusion of the copolymer of methyl vinyl ether and maleic anhydride decreased the surface area of Si-MCM-41, whereas the inclusion of the tartrate led to Si-MCM-41 with a similar S<sub>BET</sub> to the material whose CTAB solution was not influenced by any additive (the TEM micrograph of this sample, Figure 2.31, also suggests order in the channel system). The difference between the templating mechanisms of these two additives may stem from the ionic charges associated with their molecules, which would consequently interact the cationic surfactant template and the anionic silicate precursor (sodium silicate).

Table 2.6 The effect of additives to the synthesis gel on the surface area of Si-MCM-41

Surfactant type	$a_0/\text{Å}$	SA ( $\text{m}^2/\text{g}$ )
C <sub>16</sub> TMAB	46.8	988
C <sub>16</sub> TMAB + copol <sup>a</sup>	45.4	731
C <sub>16</sub> TMAB + tartrate <sup>b</sup>	47.1	995

<sup>a</sup>Copolymer of methyl vinyl ether and maleic anhydride added to the synthesis gel

<sup>b</sup>Sodium potassium tartrate added to the synthesis gel

As a means of enhancing or improving the order properties of Si-MCM-41 and its resulting textural properties, a composite silica source was made by mixing TEOS and water glass with varying SiO<sub>2</sub> molar contributions, prior to gelation and hydrothermal treatment at 80 °C for 6 h. The mole ratio of the silica contributions from the two sources is shortened  $R_{\text{SiO}_2}$ , and is defined as  $R_{\text{SiO}_2} = \text{mol SiO}_2 (\text{TEOS})/\text{mol SiO}_2 (\text{water-glass})$ . Analysis of the resulting pure silica samples by BET surface area measurement gave the data summarized in Table 2.7.

Table 2.7 Effect of gel  $R_{\text{SiO}_2}$  on  $S_{\text{BET}}$  of Si-MCM-41

$R_{\text{SiO}_2}$	$S_{\text{BET}} (\text{m}^2/\text{g})$
0	1225
1.48	1225
3.95	1104
5.53	903
11.84	786
28.49	1109

It is apparent from the table above that Si-MCM-41 materials made from a composite silica source exhibit excellent mesoporous properties in the context of the  $S_{\text{BET}}$ 's.

Another noteworthy feature from the data is that the sodium silicate determines or plays a major role in giving high surface area materials. It can also be seen from this table that the mesoporous properties of the resulting material decrease with an increase in the  $R_{\text{SiO}_2}$  value up to 11.84 and then resumes beyond this point. The XRD patterns (*appendix A.1*) of these materials also supports the BET surface area data given in the above table. The long-range order is progressively lost on lowering the amount of added sodium silicate. It can be concluded from this observation that the sodium silicate not only plays a gelling role, but also serves as a structural promoter because the degree of ordering of mesopores increases with increasing sodium silicate content of the synthesis mixture. However, equimolar silica contributions from the two sources results in a material with the surface area equal to the one obtained using water glass as the sole silica source. This confirms the statement made above that the water glass seems to be responsible for the integrity of the resulting mesoporous material, or is a primary framework former. The breakdown in the trend in surface area at a ratio of 28.49 can be attributed to the formation of an amorphous phase as the TEOS, which is essentially electrically neutral and interact remotely with the cationic surfactant, is the dominating  $\text{SiO}_2$  source. This table, together with figure 2.34, suggest that the optimum ratio of the silica contributions from the two sources for the production of a highly ordered materials is  $R_{\text{SiO}_2} = 3.95$ .

### **2.3.3 High Resolution Transmission Electron Microscopy (HRTEM) studies**

HRTEM has been used to study the microstructure of Si-MCM-41 materials after calcination. Figure 2.30 below shows the porous structure of pure silica MCM-41 synthesized hydrothermally at 100 °C for 5 days.

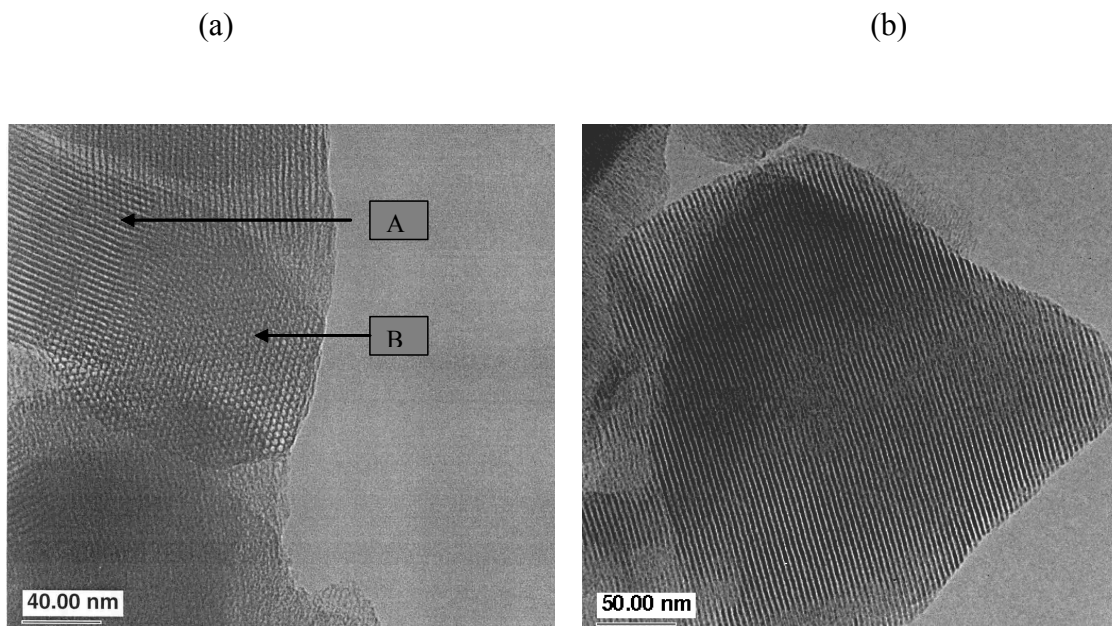


Figure 2.30. HRTEM images of Si-MCM-41 prepared at 100 °C for 5 days, and calcined at 560 °C for 6 h

Figure 2.30(a) shows a hexagonal array of regular channels consistent with literature reports [6, 7]. The labeled portions show that the electron beam can be perpendicular to the pore direction (region A), and parallel to the pore (region B). Both regions show regularity, with region A exhibiting a regular interpore distance, whereas region B exhibits a regular pore size or diameter. Thus the mesostructure of Si-MCM-41 can be seen under HRTEM as tubes or channels/pores depending on the orientation of the microscope electron beam. Figure 2.30 (a) shows, in addition, an amorphous portion near the bottom of the micrograph. This further confirms the amorphousness suggested in Figures 2.14 and 2.29. Figure 2.30 (b) shows predominantly the MCM-41 tubes, where an electron beam is perpendicular to the direction of the pore. The tubes are also highly ordered as can be deduced from the distance between two adjacent tubes (Figure 2.30 (b)).

The inclusion of sodium potassium tartrate in the template (CTAB) solution and carrying out the hydrothermal synthesis (100 °C 2 d) of Si-MCM-41 under unstirred

conditions has also been found to afford a highly ordered mesoporous material. Figure 2.31 below shows the micrographs of the resulting material after calcination at 560 °C for 6 h.

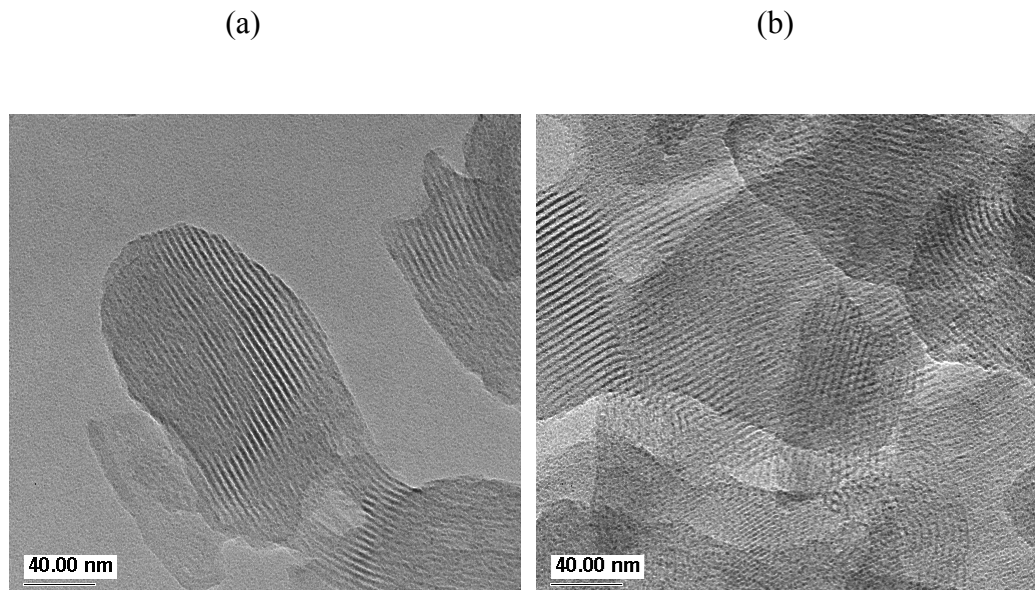


Figure 2.31. HRTEM images of Si-MCM-41 made with CTAB/NaK-tartrate as template, calcined at 560 °C for 6 h: Images taken at different regions of the same sample.

Noticeably, the alignment of the pores in this material is mostly perpendicular to the electron beam direction, making the mesostructure appear as ropes. However, regardless of the orientation, the channels show increased regularity. The BET surface area (995 m<sup>2</sup>/g in Table 2.6) measurement on this material also supports this high degree of order in the mesopore system.

Changing the surfactant template from CTAB to C<sub>14</sub>TMAB (i.e., from 16-C to 14-C surfactant), and carrying out the synthesis at 100 °C for 2 days also afforded good Si-MCM-41 materials. Figure 2.32 below illustrates the pore ordering in the resulting calcined (560 °C, 6 h).

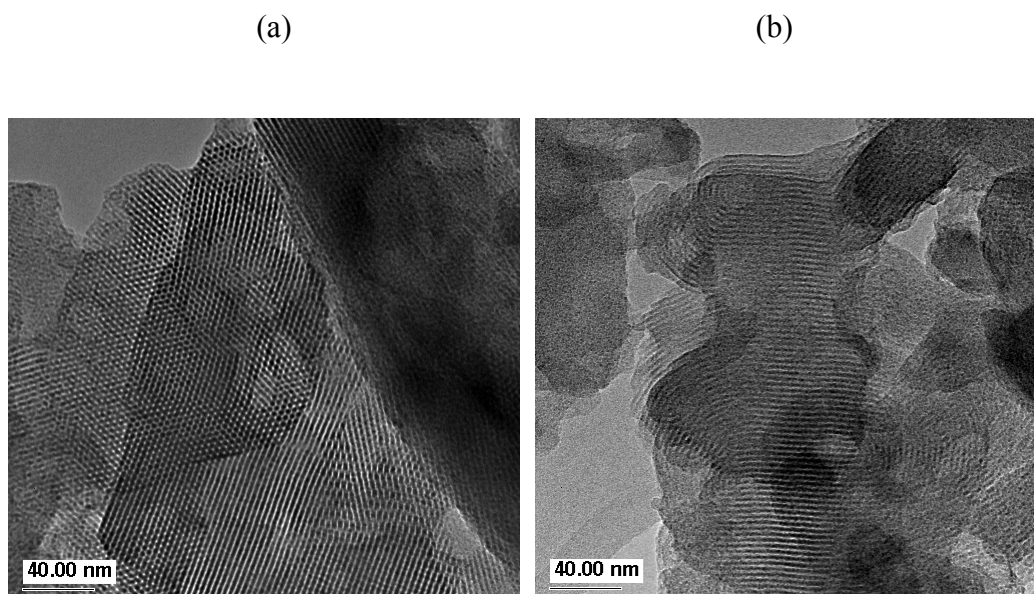


Figure 2.32. Different regions of Si-MCM-41 (2 days, 100 °C, C<sub>14</sub>TMAB as template, calcined at 560 °C for 6 h) as seen under HRTEM

The two images above, taken from different regions of the same sample, also show order in the pores and channels, with the channels (right micrograph) resembling an onion slice. In fact, Figure 2.32 (b) shows that the mesopores are not necessarily running in a straight pattern through the silica matrix, but can be slightly curved with retention of the hexagonal ordering.

Highly porous mesoporous Si-MCM-41 materials have also been obtained at relatively lower synthesis temperature (80 °C) under magnetic stirring, over a short synthesis time (6 h). These materials were prepared using a compound silica source comprising water glass and TEOS, although incremental amounts of water glass were added at a fixed amount of TEOS (total silica content also fixed). Figure 2.33 shows two regions of the same Si-MCM-41 sample having the silica contributions  $R_{\text{SiO}_2} = 3.95$ .

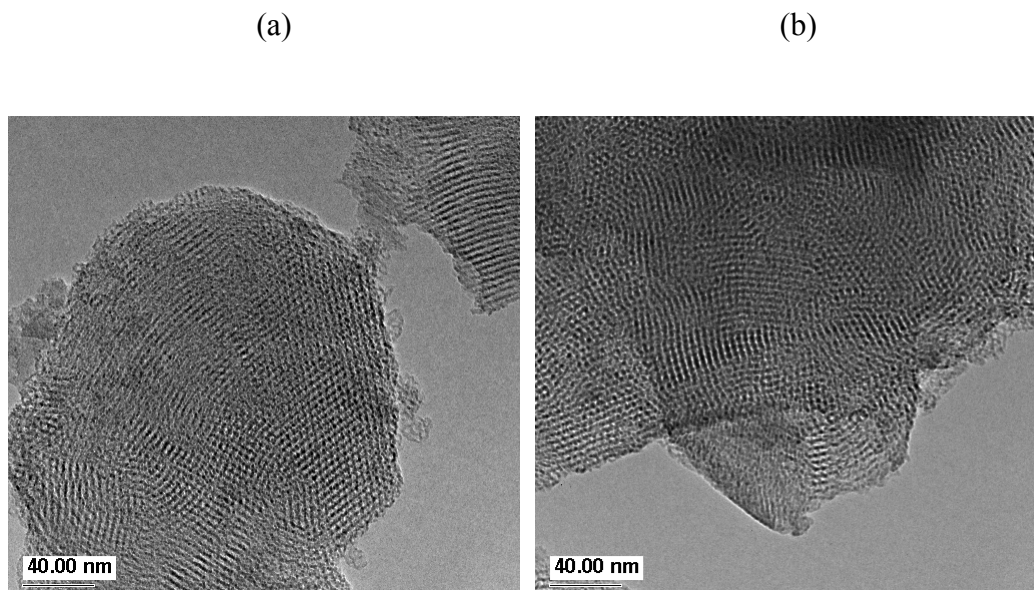


Figure 2.33. HRTEM images of different regions of Si-MCM-41 prepared at 80 °C for 6 h,  $R_{\text{SiO}_2} = 3.95$ , and calcined at 500 °C for 12 h.

It can be seen from the above figure that the resulting material prepared through this method is highly porous, with the pores characteristic of MCM-41, both in shape and regularity. The left micrograph shows both pores and channels relative to the electron beam direction. Therefore, Si-MCM-41 can be obtained both at lower temperatures (compared to 100 °C) over reduced synthesis time, while keeping or retaining the high long-range order of the pores.

Decreasing the  $R_{\text{SiO}_2}$  molar ratio of the synthesis gel to 1.48 and carrying out the synthesis as above, yields a material with the microstructure depicted in Figure 2.34 below. This Si-MCM-41 material possesses long-range order in the channel structure (*cf. XRD patterns in appendix A.1*). However, the porosity is inferior compared to that of the material reported in Figure 2.33 above (with  $R_{\text{SiO}_2} = 3.95$ ). The surface areas of these two materials (see Table 2.7 above) made from gels of similar compositions but different sodium silicate contents, may suggest the existence of an

optimum ratio ( $R_{\text{SiO}_2}$ ) for the synthesis of highly porous and highly ordered Si-MCM-41 with a high BET surface area under these conditions.

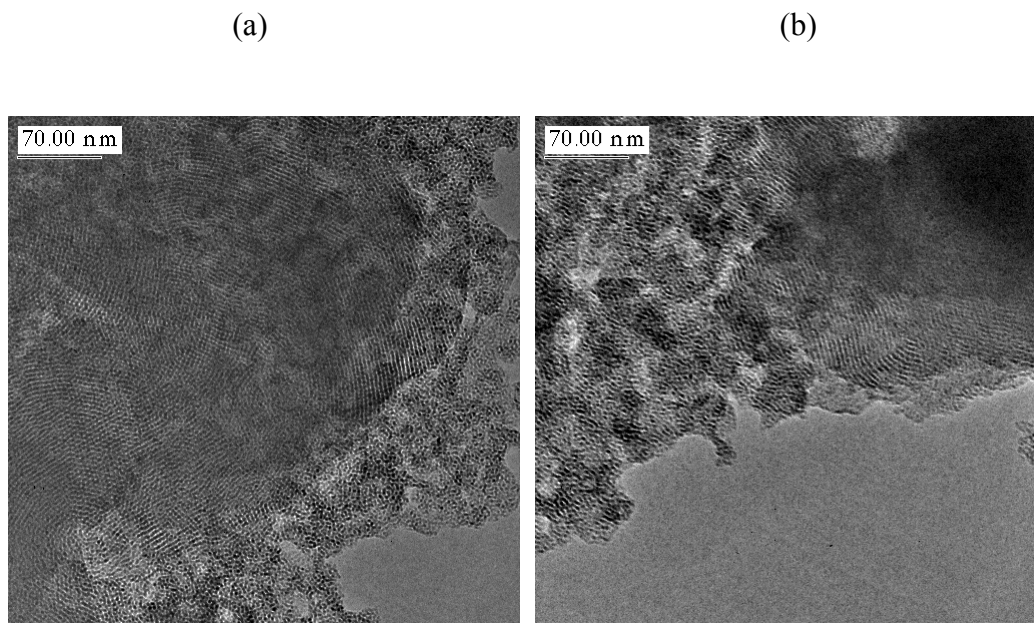


Figure 2.34. HRTEM images of different regions of Si-MCM-41 prepared at 80 °C for 6 h, with  $R_{\text{SiO}_2} = 1.48$ , and calcined at 500 °C for 12 h.

## 2.4 Conclusions

Si-MCM-41 materials have been successfully synthesized following the modified “delayed neutralization” method. These materials were characterized by using three principal techniques that provide unambiguous evidence regarding the quality of mesoporous materials, viz., XRD, BET surface area measurements and HRTEM. All samples synthesized showed a prominent  $d_{100}$  reflection around  $2.2^\circ 2\theta$  in their XRD patterns, BET surface areas in the vicinity of  $1000 \text{ m}^2/\text{g}$ , and a regular array of hexagonal channels in their TEM images.

A wide range of synthesis variables has been investigated for their possible impact on the quality of the resulting Si-MCM-41, with the aim of finding optimum synthesis conditions. This optimization process was done both for the room-temperature synthesis and for the hydrothermal synthesis.

### *Room Temperature Synthesis of Si-MCM-41*

For room temperature synthesis, these synthesis variables investigated included: (i) the synthesis time, (ii) the alkyl chain length of the surfactant template, (iii) the  $\text{SiO}_2$  to CTAB molar ratio of the synthesis gel, (iv) the  $\text{H}_2\text{O}$  to  $\text{SiO}_2$  molar ratio of the synthesis gel, (v) secondary synthesis and (vi) acid identity in pH adjustment. Room temperature synthesis has been found to give rise to a highly ordered pure silica MCM-41 material, although longer crystallization periods are required. Importantly, the lattice parameters ( $a_0$ ) of the materials synthesized at ambient do not show significant variation with the synthesis time, with the relative error of  $\sim 1.6\%$  between the values. The lattice parameters for these ambient-synthesized materials also showed variation with the surfactant template alkyl chain length ( $a_0$  values of  $44.0 \text{ \AA}$  for CTAB and  $38.0 \text{ \AA}$  for  $\text{C}_{14}\text{TMAB}$ ) in accordance with literature reports [6, 7]. However, the use of a mixture of these two surfactants to template the room temperature synthesis of Si-MCM-41 produced a material with a lattice parameter

intermediate between the above two values [42.0 Å]. In contrast to the findings by Vartuli et al [13], who could obtain Si-MCM-41 at a gel CTAB/SiO<sub>2</sub> molar ratio of 1 under hydrothermal conditions, our approach yielded reasonably good quality Si-MCM-41 in the composition range  $0.125 \leq \text{CTAB/SiO}_2 \leq 0.800$  at room temperature. The trend in the data suggests that CTAB/SiO<sub>2</sub> = 0.308 is the optimum composition for achieving an ordered material at room temperature.

The synthesis gel water content in the range  $42 \leq \text{H}_2\text{O/SiO}_2 \leq 140$  had little influence on the lattice parameters of the resulting Si-MCM-41, with the mean lattice parameter of 44.2 Å. Although the  $S_{\text{BET}}$  of the materials synthesized at room temperature showed no specific trend, they were all very high and characteristic of MCM-41-type materials. Notably, the materials prepared at room temperature were found to have higher specific surface areas than their hydrothermal counterparts, regardless of the H<sub>2</sub>O/SiO<sub>2</sub> ratio of the synthesis gel.

Secondary Si-MCM-41 synthesized at room temperature over two days showed a lattice contraction of ~3.9 % relative to the parent siliceous material, which can be associated with the increased crystallinity of the pore wall and consequent thickening upon secondary synthesis.

### ***Hydrothermal Synthesis of Si-MCM-41***

More synthesis parameters have been investigated in the hydrothermal synthesis of Si-MCM-41 than there were in room temperature synthesis. This is because the room temperature synthesis was just meant for screening the workable synthesis composition, as zeolite synthesis is mostly a high temperature-high pressure reaction. The variables in this section included: (i) the synthesis temperature, (ii) the synthesis gel pH, (iii) the synthesis time, the H<sub>2</sub>O/SiO<sub>2</sub> molar ratio of the synthesis gel, (iv) the nature of the solvent, (v) the reproducibility or reliability of the synthesis method, (vi) the identity of the mineral acid (in pH adjustment), (vii) secondary synthesis, (viii)

the identity of the silica source, and (ix) the structural contraction upon calcination. Hydrothermal synthesis has been found to give rise to siliceous materials of superior quality (XRD patterns) than similar materials prepared at room temperature. At least four diffraction peaks were observed in the XRD patterns of these materials, assignable to the (100), (110), (200) and the (210) reflection planes. This superior quality of the hydrothermally-synthesized materials may stem from the enhanced condensation of the silanol groups and the consequent polymerization of the silicate species under hydrothermal conditions. The best synthesis conditions for the preparation of good quality Si-MCM-41 was found to be a temperature of 100 °C, a crystallization time of 2-3 days (giving samples with lattice parameters of 46.9 and 47.1 Å for 2 and 3 days, respectively), and a synthesis gel of pH 10. Very low pH values (pH 2) and very high pH values (pH 14) of the synthesis gel prior synthesis have shown to be detrimental to the quality of the Si-MCM-41 product, as revealed by XRD patterns (Fig. 2.11). Also, prolonged crystallization time (beyond 3 days) led to a reduction in the lattice parameter of the resulting Si-MCM-41 material, possibly due to partial solubility of the already formed product in its alkaline mother liquor.

Replacing the distilled water solvent with a pH 10 buffer solution for the hydrothermal synthesis (100 °C 2 d) of Si-MCM-41, resulted in a material that was highly ordered even in the as-synthesized state (revealed by the appearance of the (300) peak in the XRD pattern).

The lattice parameter of Si-MCM-41 synthesized under hydrothermal conditions is insensitive to the water content of the synthesis gel ( $a_0 \approx 47$  Å). Remarkably, the hydrothermally-synthesized materials possess higher lattice parameters and are more ordered than those prepared at ambient temperatures with the same synthesis gel water content.

The synthesis approach adopted in this study (100 °C for 2 days) is highly reproducible, and also highly versatile because larger batches of Si-MCM-41 can be synthesiz-

ed under hydrothermal conditions without jeopardizing the structural integrity of the material.

The as-synthesized forms of primary and secondary Si-MCM-41 both undergo lattice contraction (see the reduction in the lattice parameter ( $a_0$ )) upon calcination at 560 °C. In addition, the extent of contraction is more pronounced after calcination at 850 °C as compared to calcination at 560 °C. This reduction is associated with the relaxation of the pore as the pillaring agent (the occluded template) burns off, and the pore diameter shrinks as a consequence. The fact that the material was still mesoporous (XRD) after this high temperature calcination suggests increased thermal stability of materials prepared via secondary crystallization.

The extent of secondary crystallization does not have a significant effect on the decrease in pore size of the *sec*-Si-MCM-41 relative to the parent Si-MCM-41 sample. Secondary Si-MCM-41 synthesized over four days under hydrothermal conditions (100 °C) showed ~4.9 % reduction in  $a_0$  while that prepared over two days synthesis showed a 4.6 % contraction upon calcination at 560 °C. In each case, the reduction in the lattice parameter has been associated with pore-wall thickening. The fact that primary Si-MCM-41 undergoes a 5.5 % lattice contraction upon calcination reveals the amorphous nature of its walls, which get strengthened upon secondary synthesis. The high long-range order in the *sec*-Si-MCM-41 prepared at 100 °C was revealed by the appearance of the (300) diffraction peak.

The dependence of the quality of Si-MCM-41 on the nature of the SiO<sub>2</sub> source has been demonstrated, and the order of decreasing quality as a function of SiO<sub>2</sub> source is: Si-MCM-41 > (Water-glass + Fumed SiO<sub>2</sub>) > Water-glass >>TEOS.

Due to the closeness of in ionic size between Al<sup>3+</sup> and Si<sup>4+</sup>, the Al-containing MCM-41 did not show any marked structural difference from Si-MCM-41.

Regardless of the synthesis temperature under hydrothermal conditions and the extent of hydrothermal treatment, the BET surface areas of the resulting Si-MCM-41 remained essentially high. These high surface areas were also not too sensitive to the  $\text{H}_2\text{O}/\text{SiO}_2$  ratio of the synthesis gel. Importantly, regardless of the water content, the room temperature synthesis gave materials with higher BET surface areas than those obtained from hydrothermal synthesis (the highest  $S_{\text{BET}}$  for Si-MCM-41 made at room temperature in this study was  $1344 \text{ m}^2 \cdot \text{g}^{-1}$ ).

Siliceous MCM-41 prepared at  $80 \text{ }^\circ\text{C}$  for 6 h under magnetic stirring, from a compound  $\text{SiO}_2$  source (i.e., TEOS + water-glass), also possessed extremely high surface areas characteristic of mesoporous materials. These BET areas decreased with decreasing water-glass content of the synthesis gel, suggesting that water-glass is the primary framework former (because of charge matching with the cationic template) and induces the polymerization of TEOS. The XRD patterns (*see appendix A.1*) show a decrease in structural order and loss of the hexagonal symmetry when the water-glass content is significantly reduced, i.e., at higher  $R_{\text{SiO}_2}$  values.

HRTEM micrographs of the Si-MCM-41 prepared from single and compound silica sources show a regular array of hexagonal 1-D pores and channels running parallel to each other. Channels similar to onion slices have also been observed in micrographs of certain materials (Figure 2.32).

## 2.5 References

1. IUPAC, Manual of Symbols and Terminology, *Pure Appl. Chem.* **31**, 578 (1972); K.S. W. Sing, D. H. Everett, R. H. W. Haul, L. Moscou, R. A. Pierotti, J. Rouquerol and T. Siemieniewska, *Pure Appl. Chem.* **57**, 603 (1985)
2. R. K. Iler, in: *The Chemistry of Silica*, John Wiley & Sons, Inc., New York, (1979)
3. T. J. Pinnavaia, *Science* **220**, 365 (1983)
4. M. E. Landis et al, *J. Am. Chem. Soc.* **113**, 3189 (1991)
5. R. M. Tindwa, D. K. Ellis, G. Z. Peng and A. Clearfield, *J. Chem. Soc., Faraday Trans. 1*, **81**, 545 (1985)
6. Kresge et al, *Nature* **359**, 710 (1992)
7. J. S. Beck et al, *J. Am. Chem. Soc.* **114**, 10834 (1992)
8. T. Yanagisawa, T. Shimizu, K. Kuroda and C. Kato, *Bull. Chem. Soc. Jpn.* **63**, 988 (1990)
9. S. Inagaki, Y. Fukushima and K. Kuroda, *J. Chem. Soc., Chem. Commun.* 680 (1993)
10. U. Ciesla and F. Schuth, *Microp. Mesop. Mater.* **27**, 131, (1999)
11. C. J. Brinker and G. W. Scherer, *Sol-Gel Science: The Physics and Chemistry of Sol-Gel Processing*, Academic Press, NY, (1990)
12. D.-W. Hua, *Environmental Study of Physical-Chemical Factors in Sol-Gel Process*, Thesis (University of Illinois at Urbana-Champaign, IL, (1991)
13. J. C. Vartuli, K. D. Schmitt, C. T. Kresge, W. J. Roth, M. E. Leonowicz, S. B. McCullen, S. D. Hellring, J. S. Beck, J. L. Schlenker, D. H. Olson and E. W. Sheppard, *Chem. Mater.* **6**, 2317 (1994)

14. K. J. Edler and J. W. White, *Chem. Mater.* **9**, 1226 (1997)
15. C.-F. Cheng, D. H. Park and J. Klinowski, *J. Chem. Soc., Faraday Trans.*, **93** (1), 193 (1997)
16. A. Monnier et al, *Science* **261**, 1299 (1993)
17. A. Wang and T. Kabe, *Chem. Commun.* 2067, (1999)
18. R. Mokaya, *J. Phys. Chem. B* **103**, 10204 (1999)
19. R. Mokaya, W. Zhou and W. Jones, *J. Mater. Chem.* **10**, 1139 (2000)
20. H.-P. Lin, S. Cheng and C.-Y. Mou, *Micropor. Mater.* **10**, 111 (1997)
21. H.-P. Lin, S. Cheng and C.-Y. Mou, *J. Chin. Chem. Soc.*, **43**, 375, (1996)
22. H.-P. Lin, Y.-R. Cheng, C.-R. Lin, F.-Y. Li, C.-L. Chen, S.-T. Wong, S. Cheng, S.-B. Liu, B.-Z. Wan, C.-Y. Mou, C.-Y. Tang and C.-Y. Wan, *J. Chin. Chem. Soc.*, **46**, 495 (1999)
23. J. M. Kim, J. H. Kwak, S. Jun and R. Ryoo, *J. Phys. Chem.* **99**, 16742 (1995)
24. R. Ryoo and J. M. Kim, *J. Chem. Soc., Chem. Commun.* 711 (1995)
25. J. M. Kim and R. Ryoo, *Bull. Korean Chem. Soc.* **17**, 66 (1996)
26. K. J. Edler and J. W. White, *J. Mater. Chem.* **9**, 2611, (1999)
27. R. Mokaya, W. Zhou and W. Jones, *Chem. Commun.* 51 (1999)
28. R. Mokaya, *Micropor. Mesopor. Mater.* **44-45**, 119 (2001)
29. K. W. Gallis and C. C. Landry, *Chem. Mater.* **9**(10), 2035 (1997)
30. R. Ryoo and S. Jun, *J. Phys. Chem.* **101**, 317 (1997)
31. C.-Y. Chen, H.-X. Li and M. E. Davis, *Microporous Mater.* **2**, 17 (1993)
32. C.-Y. Chen, S. L. Burkett, H.-X. Li and M. E. Davis, *Microporous Mater.* **2**, 27 (1993)

33. C.-Y. Chen, S.-Q. Xiao and M. E. Davis, *Microporous Mater.* **4**, 1 (1995)
34. M. Janicke, D. Kumar, G. D. Stucky and B. F. Chmelka: In *Zeolites and Related Materials: State of the Art 1994*; J. Weitkamp et al, eds.; Studies in Surface Science and Catalysis, Vol. 84, Elsevier, Amsterdam, 1994, pp 243-250